

KGS
OF
83-34

FINITE DIFFERENCE SOLUTION OF UNSTEADY STREAM FLOW

Marian Kemblowski

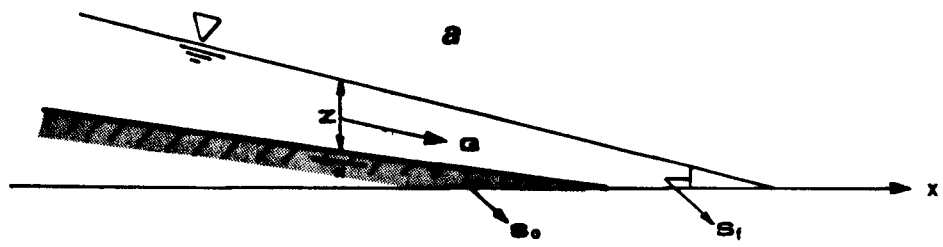
ABSTRACT

This report presents a finite difference solution and the numerical program for simulating the unsteady stream flow described by Saint-Venant's equations. The model is both general and flexible and can be applied to a wide range of problems. The model computes changes in stream stage and stream discharge caused by changes in boundary conditions and lateral discharge. The boundary conditions included in this model are: stage or discharge hydrographs as the upper boundary condition (beginning of the stream reach under consideration) and Manning's equation at the end of the reach as the lower boundary. The model includes the influence of groundwater discharge into a stream or stream water infiltration into an aquifer upon stream stage and discharge.

Finite difference formulation of the Saint-Venant's equations leads to a system of non-linear equations. This system is solved using Newton's method.

This report includes a listing of the computer program and user's manual.

Figure 1. One-dimensional stream flow. (a) Longitudinal section.
(b) Cross section.



b

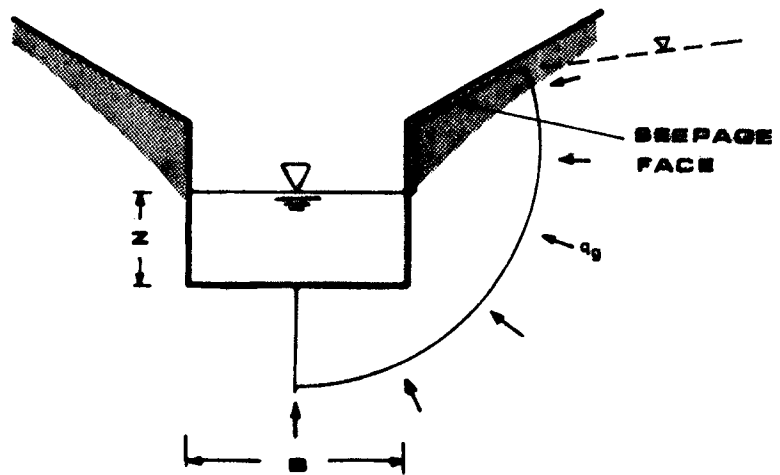


Figure 1

SAINT-VENANT EQUATIONS

The Saint-Venant equations describe the one-dimensional unsteady, spatially varied flow of a homogeneous liquid in a rigid channel of arbitrary shape and alignment. This pair of equations, one based on conservation of mass (continuity), the other on conservation of either energy or momentum, has only two unknown dependent variables, depth of flow and discharge (assuming channel geometry and lateral discharge are known). These equations provide a system which can be solved simultaneously, once the appropriate initial and boundary conditions have been specified.

The one-dimensional partial differential equations of gradually varied, unsteady channel flow, known as Saint-Venant equations, represent equations of continuity and motion, respectively, as follows (Strelkoff, 1969):

$$\frac{\partial Q}{\partial x} + B \frac{\partial z}{\partial t} - q = 0 \quad (1)$$

$$\frac{1}{g} \frac{\partial Q/A}{\partial t} + \frac{Q/A}{g} \frac{\partial Q/A}{\partial x} + \frac{\partial z}{\partial x} - S_o + S_f + D_L = 0 \quad (2)$$

where

| | |
|--|----------------|
| Q = discharge across a channel section | $[L^3 T^{-1}]$ |
| A = cross sectional area of flow | $[L^2]$ |
| z = depth of flow normal to the bottom | $[L]$ |
| $B = \partial A / \partial z$ = the top width of the cross section for the depth z | $[L]$ |
| q = lateral inflow ($q < 0$ for outflow) | $[L^2 T^{-1}]$ |
| g = gravitational acceleration | $[L^2 T^{-1}]$ |
| S_o = longitudinal slope of the channel bottom | $[L^0]$ |
| S_f = friction slope defined as | $[L^0]$ |

$$S_f = n^2 Q |Q| / (NA^2 R^{4/3}) \quad (3)$$

n = Manning's roughness coefficient [-]

P = wetted perimeter of the channel [L]

N = conversion factor taking the value of $1 \text{ m}^{2/3}/\text{s}^2$ for S.I. [$L^{2/3}T^{-2}$]

and

$$D_L = 0 \text{ (bulk lateral outflow)} \quad (4a)$$

$$D_L = \frac{Qq}{2gA^2} \text{ (seepage outflow)} \quad (4b)$$

$$D_L = \frac{Q/A - u_x}{Ag} q \text{ (lateral inflow)} \quad (4c)$$

in which u_x = the average component of inflow velocity in

the x direction

[LT^{-1}]

Equations 1 and 2 are subject to the initial and boundary conditions. For the present work, the upper boundary condition may be either stage or discharge hydrograph. The lower boundary is expressed by a rating curve. For this study, the rating curve is assumed to be described by the Manning equation as follows (Henderson, 1966):

$$Q = \frac{A \cdot R^{2/3} \sqrt{S_o}}{n} \quad (5)$$

Initial conditions employed are those of steady-state flow. In the numerical program both Q and z are assumed known initially.

FINITE DIFFERENCE APPROXIMATION

Finite difference method is based on replacing partial derivatives by difference quotients. In this way the original partial differential equations are transformed into an algebraic system. It is clear that by adopting different approximations for partial derivatives and the coefficients, different numerical systems are obtained.

The numerical grid, on the vertices of which the values of unknowns are computed, together with the system of difference equations, form the so-called difference scheme.

Referring to the computation grid of Figure 2, the following general approximations of a quantity, for example the flow depth z , and its derivatives, may be written (Greco and Panattoni, 1977)

$$z_{i,j+1}^{k,k+1} \approx \psi \phi z_{i+1}^{k+1} + (1 - \psi) \phi z_i^{k+1} + \psi(1 - \phi) z_{i+1}^k + (1 - \psi)(1 - \phi) z_i^k \quad (6)$$

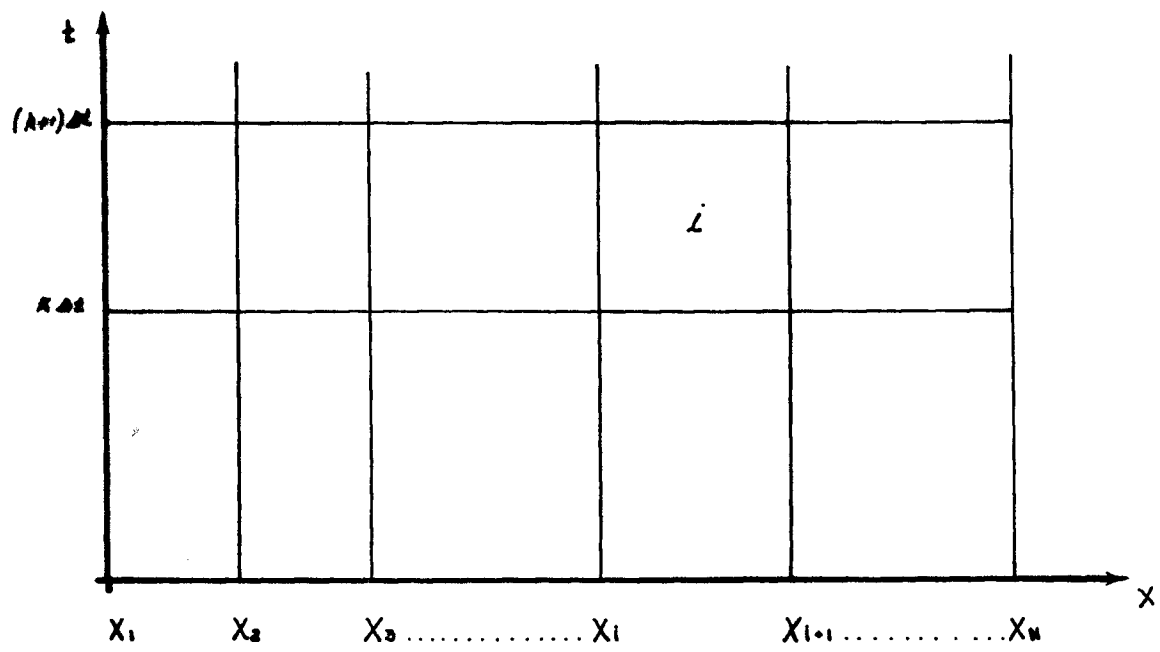


Figure 2

Figure 2. Computation grid.

$$\frac{\partial z}{\partial x} \approx \frac{\phi}{\Delta t} (z_{i+1}^{k+1} - z_i^{k+1}) + \frac{1 - \phi}{\Delta x} (z_{i+1}^k - z_i^k) \quad (7)$$

$$\frac{\partial z}{\partial t} \approx \frac{\psi}{\Delta t} (z_{i+1}^{k+1} - z_{i+1}^k) + \frac{1 - \psi}{\Delta x} (z_i^{k+1} - z_i^k) \quad (8)$$

in which the upper index (k) refers to time and lower (i) refers to space. In these formulae ψ and ϕ are weighting coefficients between 0 and 1 with which the different variables and their derivatives are averaged with respect to space (ψ) and time (ϕ).

In this study the following values of the weighting coefficients are assumed: $\psi = 0.5$; $\phi = 1.0$. This means that a fully implicit scheme is used. In this way there are no restrictions for the time (Δt) and space (Δx) intervals, and, furthermore, it is possible to fit the computational grid to the experimental data.

FINITE DIFFERENCE SOLUTION OF SAINT-VENANT EQUATIONS WITHOUT LATERAL DISCHARGE

The one-dimensional partial differential equations of gradually varied, unsteady channel flow without lateral discharge are given by:

$$\frac{\partial Q}{\partial x} + B \frac{\partial z}{\partial t} = 0 \quad (9)$$

$$\frac{\partial z}{\partial x} - S_o + S_f + \frac{1}{g} \left[\frac{\partial Q/A}{\partial t} + \frac{Q}{A} \frac{\partial Q/A}{\partial x} \right] = 0 \quad (10)$$

Applying the finite difference approximation, given by eqs. 6, 7, and 8, with the weighting coefficient $\psi = 0.5$ and $\phi = 1.0$, leads to the equations

$$G_i \equiv Q_{i+1}^{k+1} - Q_i^{k+1} + \frac{B_i^{k+1} + B_{i+1}^{k+1}}{2} \frac{\Delta x_i}{2\Delta t} (z_i^{k+1} - z_i^k + z_{i+1}^{k+1} - z_{i+1}^k) = 0 \quad (11)$$

$$\begin{aligned} F_i \equiv & z_{i+1}^{k+1} - z_i^{k+1} + \frac{\Delta x_i}{2} (S_{f_i}^{k+1} + S_{f_{i+1}}^{k+1} - S_{o_i} - S_{o_{i+1}}) \\ & + \frac{\Delta x_i}{2g\Delta t} \left[\frac{Q_{i+1}^{k+1}}{A_{i+1}^{k+1}} - \frac{Q_{i+1}^k}{A_{i+1}^k} + \frac{Q_i^{k+1}}{A_i^{k+1}} - \frac{Q_i^k}{A_i^k} \right] \\ & + \frac{1}{2g} \left[\frac{Q_{i+1}^{k+1}}{A_{i+1}^{k+1}} + \frac{Q_i^{k+1}}{A_i^{k+1}} \right] \left[\frac{Q_{i+1}^{k+1}}{A_{i+1}^{k+1}} - \frac{Q_i^{k+1}}{A_i^{k+1}} \right] \end{aligned} \quad (12)$$

in which $\Delta x_i = x_{i+1} - x_i$.

For simplicity, from this point onward, the variables without upper indices refer to the time $(k+1) \Delta t$.

Equations 11 and 13 contain four unknown variables:

$$Q_{i+1}^{k+1}, Q_i^{k+1}, z_i^{k+1}, z_{i+1}^{k+1}.$$

These equations form a system of algebraic equations, whose solution gives the values of stage and discharge at nodes at the time $(k+1)\Delta t$. These values form the initial conditions for the next time step. Solution of this system utilizes the Arno method (Greco and Panattoni, 1977). This method exploits the linearity in the discharge of the continuity equation. The continuity equation may be written for the discharge at the node i as follows:

$$Q_i = Q_{i+1} + f(z_i, z_{i+1}) \quad (13)$$

Using this equation for all grid nodes, it is possible to express the discharge at any node as a function of the discharge Q_N at the extreme node (lower boundary) and of the flow depths at all nodes between them. This function is given by:

$$Q_i = Q_N + g(z_i, z_{i+1}, \dots, z_N) = Q_i(z_i, z_{i+1}, \dots, z_N, Q_N) \quad (14)$$

Replacing the discharge value in eq. 12 with eq. 14 gives

$$f_i \equiv F_i(z_i, z_{i+1}, Q_i(z_i, z_{i+1}, \dots, z_N, Q_N), Q_{i+1}(z_{i+1}, \dots, z_N, Q_N)) = 0 \quad (15)$$

By applying this equation at the N-1 nodes, the following system of N-1 equations for N+1 unknowns $z_1, z_2, \dots, z_N, Q_N$ is obtained:

$$\begin{aligned} f_1(z_1, z_2, \dots, z_N, Q_N) &= 0 \\ f_2(z_2, z_3, \dots, z_N, Q_N) &= 0 \\ f_{N-1}(z_{N-1}, z_N, Q_N) &= 0 \end{aligned} \tag{16}$$

The additional two equations necessary to solve this system are given by the boundary conditions. In this study we assume that the lower boundary condition is given by the rating curve, as follows:

$$f_N(z_N, Q_N) = 0 \tag{17}$$

The upper boundary condition is given either by the stage hydrograph or by the discharge hydrograph. In the former case, the value z_1 is given explicitly as a known variable. In the latter case, the additional equation of mass conservation at the first node may be written

$$f_0 = Q_N - Q_1 + \frac{1}{2\Delta t} \sum_{j=1}^{N-1} \frac{B_j + B_{j+1}}{2} \Delta x_j (z_j^{k+1} + z_{j+1}^{k+1} - z_{j+1}^k - z_j^k) = 0 \tag{18}$$

Equations 16, 17, and 18 (for the discharge hydrograph) form a system of non-linear equations. In order to solve this system, the Newton iterative method is used (Macon, 1963). For the system of equations given by

$$f_i(\{x\}) = 0 \quad i = 1, 2, \dots, N \tag{19}$$

where the components for $i = 1, 2, \dots, N-1$ are:

$$b_i = \frac{\partial f_i}{\partial z_i} = \frac{\partial F_i}{\partial z_i} + \frac{\partial F_i}{\partial S_{fi}} \frac{\partial S_{fi}}{\partial z_i} + \frac{\partial F_i}{\partial A_i} \frac{\partial A_i}{\partial z_i} + \left(\frac{\partial F_i}{\partial Q_i} + \frac{\partial F_i}{\partial S_{fi}} \frac{\partial S_{fi}}{\partial Q_i} \right) \frac{\partial Q_i}{\partial z_i} \quad (23)$$

$$\begin{aligned}
a_i \equiv \frac{\partial f_i}{\partial z_{i+1}} &= \frac{\partial F_i}{\partial z_{i+1}} + \frac{\partial F_i}{\partial S_{fi+1}} \frac{\partial S_{fi+1}}{\partial z_{i+1}} + \frac{\partial F_i}{\partial A_{i+1}} \frac{\partial A_{i+1}}{\partial z_{i+1}} \\
&+ \left(\frac{\partial F_i}{\partial Q_i} + \frac{\partial F_i}{\partial S_{fi}} \frac{\partial S_{fi}}{\partial Q_i} \right) \frac{\partial Q_i}{\partial z_{i+1}} \\
&+ \left(\frac{\partial F_i}{\partial Q_{i+1}} + \frac{\partial F_i}{\partial S_{fi+1}} \frac{\partial S_{fi+1}}{\partial Q_{i+1}} \right) \frac{\partial Q_{i+1}}{\partial z_{i+1}}
\end{aligned} \tag{24}$$

$$\begin{aligned}
c_i \equiv \frac{\partial f_i}{\partial Q_N} &= \left(\frac{\partial F_i}{\partial Q_i} + \frac{\partial F_i}{\partial S_{fi}} \frac{\partial S_{fi}}{\partial Q_i} \right) \frac{\partial Q_i}{\partial Q_N} \\
&+ \left(\frac{\partial F_i}{\partial Q_{i+1}} + \frac{\partial F_i}{\partial S_{fi+1}} \frac{\partial S_{fi+1}}{\partial Q_{i+1}} \right) \frac{\partial Q_{i+1}}{\partial Q_N}
\end{aligned} \tag{25}$$

$$c_i d_j \equiv \frac{\partial f_i}{\partial z_j} = \frac{\partial Q_{i-1}}{\partial z_j} c_i \quad \text{for } j > i+1 \tag{26}$$

In the last equation the relationship 14 was used. From this relation, it can be deduced

$$\frac{\partial Q_i}{\partial z_i} = \frac{\partial Q_{i+1}}{\partial z_j} = \dots = \frac{\partial Q_{j-1}}{\partial z_j} \tag{27}$$

The derivatives in eqs. 23, 24, 25, and 26 are given by

$$\frac{\partial F_i}{\partial z_i} = -1 \tag{28}$$

$$\frac{\partial F_i}{\partial S_{fi}} = \frac{\Delta x_i}{2} \tag{29}$$

$$\frac{\partial F_i}{\partial A_i} = - \frac{\Delta x_i}{2g\Delta t} \left(\frac{Q_i}{A_i^2} \right) + \frac{1}{g} \frac{Q_i^2}{A_i^3} \quad (30)$$

$$\frac{\partial F_i}{\partial Q_i} = \frac{\Delta x_i}{2g\Delta t A_i} - \frac{1}{g} \frac{Q_i}{A_i^2} \quad (31)$$

$$\frac{\partial F_i}{\partial z_{i+1}} = 1 \quad (32)$$

$$\frac{\partial F_i}{\partial S_{fi+1}} = \frac{\Delta x_i}{2} \quad (33)$$

$$\frac{\partial F_i}{\partial A_{i+1}} = - \frac{\Delta x_i}{2g\Delta t} \left(\frac{Q_{i+1}}{A_{i+1}^2} \right) - \frac{Q_{i+1}^2}{gA_{i+1}^3} \quad (34)$$

$$\frac{\partial F_i}{\partial Q_{i+1}} = \frac{\Delta x_i}{2g\Delta t A_i} + \frac{Q_{i+1}}{gA_{i+1}^2} \quad (35)$$

The derivatives of discharge Q_i with respect to depth of flow z_i are calculated from eq. 14. This equation can be written as

$$Q_i = Q_N + \frac{1}{2\Delta t} \sum_{j=i}^{N-1} \frac{B_j + B_{j+1}}{2} \Delta x_i (z_i^{k+1} + z_{j+1}^{k+1} - z_j^k - z_j^k) \quad (36)$$

Thus, we can calculate

$$\frac{\partial Q_i}{\partial z_i} = \frac{\Delta x_i}{2\Delta t} \frac{B_i + B_{i+1}}{2} \quad (37)$$

$$\frac{\partial Q_i}{\partial z_{i+1}} = \sum_{j=i}^{i+1} \frac{\Delta x_j}{2\Delta t} \frac{B_j + B_{j+1}}{2} \quad (38)$$

for $i < N-1$

$$\frac{\partial Q_i}{\partial z_{i+1}} = \frac{B_i + B_{i+1}}{2} \frac{\Delta x_i}{2\Delta t} \quad \text{for } i = N-1 \quad (39)$$

The derivatives of the friction coefficient with respect to discharge and flow depth are calculated from the Manning equation. For a rectangular channel cross section this equation may be written as

$$S_f = \frac{Q|Q|n^2}{A^2 R^{4/3}} = \frac{Q|Q|n^2}{B^2 z^2 (Bz/(B+2z))^{4/3}} \quad (40)$$

Thus, we can calculate the derivatives

$$\begin{aligned} \frac{\partial S_f}{\partial z} = \frac{1}{3} Q|Q|n^2 \left[-10B^{-10/3} \cdot z^{-13/3} (B+2z)^{4/3} \right. \\ \left. + 8(Bz)^{-10/3} (B+2z)^{1/3} \right] \quad (41) \end{aligned}$$

and

$$\frac{\partial S_f}{\partial Q} = 2|Q|n^2 (B+2z)^{4/3} (Bz)^{-10/3} \quad (42)$$

For a rectangular channel cross section the derivative of the area of flow with respect to flow depth is

$$\frac{\partial A}{\partial z} = B \quad (42)$$

The last two coefficients of the matrix in eq. 22 are given by

$$b_N = \frac{\partial f_N}{\partial z_N} \quad (43)$$

and

$$a_N = \frac{\partial f_N}{\partial Q_N} \quad (44)$$

Assuming the lower boundary condition in the form of the Manning equation, we can write

$$f_N(z_N, Q_N) = Q_N - \frac{B^{5/3} z^{5/3}}{n(B + 2z)^{2/3}} S_o^{1/2} = 0 \quad (45)$$

$$a_N = \frac{B^{5/3}}{n} \sqrt{S_o} \left[-\frac{5}{3} z^{2/3} / (B + 2z)^{2/3} + \frac{4}{3} z^{5/3} / (B + 2z)^{5/3} \right] \quad (46)$$

$$b_N = 1 \quad (47)$$

$$c_{o d_j} = \sum_{i=j-1}^j \frac{\Delta x_i}{2 \Delta t} \frac{B_i + B_{i+1}}{2} \quad \text{for } j < N \quad (50)$$

$$c_{o d_N} = \frac{\Delta x_{N-1}}{2 \Delta t} \frac{B_{N-1} + B_N}{2} \quad (51)$$

$$c_o = 1 \quad (52)$$

The other components of the matrix are calculated in the same manner as in the previous section with one exception. All derivatives with respect to Q_1 are equal to zero, since this value is given by the boundary condition and does not change during the iteration process. This process is continued until eqs. 16, 17, and 18 are satisfied. Equation 36 is employed to compute the value of discharge at the nodes. As a result, we obtain the values of flow depths z_1, z_2, \dots, z_N and discharges Q_2, Q_3, \dots, Q_N for the time $(k+1)\Delta t$. These values are used as initial conditions for the next time step.

FINITE DIFFERENCE SOLUTION OF THE SAINT-VENANT EQUATIONS WITH LATERAL INFLOW TO A CHANNEL

The equations of gradually varied, unsteady channel flow with lateral inflow from an aquifer may be written as follows (Strelkoff, 1969):

$$\frac{\partial Q}{\partial x} + B \frac{\partial z}{\partial t} - q = 0 \quad (53)$$

$$\frac{1}{g} \left(\frac{\partial Q/A}{\partial t} + \frac{Q}{A} \frac{\partial Q/A}{\partial x} \right) + \frac{\partial z}{\partial x} - S_o + S_f + \frac{Q \cdot q}{A^2 g} = 0 \quad (54)$$

Cooley and Moin (1976) indicate that the term Qq/A^2g in eq. 54 may possibly lead to an unstable solution. They suggest transforming it by multiplying eq. 54 by gA and eq. 53 by Q/A , then adding the results. Eq. 54 may thus be rewritten as

$$\frac{\partial z}{\partial x} + S_f - S_o + \frac{1}{gA} \left(\frac{\partial Q}{\partial t} + \frac{\partial Q^2/A}{\partial x} \right) = 0 \quad (55)$$

or

$$\frac{\partial z}{\partial x} + S_f - S_o + \frac{1}{gA} \left(\frac{\partial Q}{\partial t} + Q \frac{\partial Q/A}{\partial x} + \frac{Q}{A} \frac{\partial Q}{\partial x} \right) = 0 \quad (56)$$

Applying the finite difference approximation given by eqs. 6, 7, and 8 with the weighting coefficient $\psi = 1/2$ and $\phi = 1$ leads to the set of equations

$$G_i \equiv Q_{i+1}^{k+1} - Q_i^{k+1} + \frac{B_{i+1}^{k+1} + B_i^{k+1}}{2} \frac{\Delta x_i}{2\Delta t} (z_i^{k+1} - z_i^k + z_{i+1}^{k+1} - z_{i+1}^k) - \frac{\Delta x_i}{2} (q_{i+1} + q_i) = 0 \quad (57)$$

$$F_i \equiv z_{i+1}^{k+1} - z_i^{k+1} + \frac{\Delta x_i}{2} (S_{fi}^{k+1} + S_{fi+1}^{k+1} - S_{oi+1} - S_{oi}) + \frac{\Delta x_i}{g\Delta t(A_{i+1}^{k+1} + A_i^{k+1})} (Q_{i+1}^{k+1} + Q_i^{k+1} - Q_{i+1}^k - Q_i^k)$$

$$+ \frac{2}{g(A_{i+1}^{k+1} + A_i^{k+1})} \left[\frac{(Q_{i+1}^{k+1})^2}{A_{i+1}^{k+1}} - \frac{(Q_i^{k+1})^2}{A_i^{k+1}} \right] = 0 \quad (58)$$

To solve this system of equations we again utilize the Arno method and Newton iterative procedure, which are described in the previous sections. The solution assumes the Manning equation at the lower boundary condition and either stage hydrograph or discharge hydrograph as the upper boundary condition.

Stage Hydrograph as the Upper Boundary Condition

Applying the Newton method to eq. 58 and utilizing the linearity of eq. 57, we obtain the system of equations given by eq. 22. The components of the matrix are calculated according to eqs. 23-47 with the following exceptions:

$$\begin{aligned} \frac{\partial F_i}{\partial A_i} = & - \frac{\Delta x_i}{g \Delta t (A_{i+1} + A_i)^2} (Q_{i+1}^{k+1} + Q_i^{k+1} - Q_{i+1}^k - Q_i^k) \\ & - \frac{2}{g(A_{i+1} + A_i)^2} \left(\frac{Q_{i+1}^2}{A_{i+1}} - \frac{Q_i^2}{A_i} \right) \\ & + \frac{2}{g(A_{i+1} + A_i)} \left(\frac{Q_i}{A_i} \right)^2 \end{aligned} \quad (59)$$

$$\frac{\partial F_i}{\partial Q_i} = \frac{\Delta x_i}{g \Delta t (A_{i+1} + A_i)} - \frac{4Q_i}{g(A_{i+1} + A_i) A_i} \quad (60)$$

$$\frac{\partial F_i}{\partial A_{i+1}} = - \frac{\Delta x_i}{g \Delta t (A_{i+1} + A_i)^2} (Q_{i+1}^{k+1} + Q_i^{k+1} - Q_{i+1}^k - Q_i^k)$$

$$\begin{aligned}
& - \frac{2}{g(A_{i+1} + A_i)^2} \left(\frac{Q_{i+1}^2}{A_{i+1}} - \frac{Q_i^2}{A_i} \right) \\
& - \frac{2}{g(A_{i+1} + A_i)} \left(\frac{Q_{i+1}}{A_{i+1}} \right)^2
\end{aligned} \tag{61}$$

$$\frac{\partial F_i}{\partial Q_{i+1}} = \frac{\Delta x_i}{g \Delta t (A_{i+1} + A_i)} + \frac{4Q_{i+1}}{g(A_{i+1} + A_i) A_{i+1}} \tag{62}$$

The iteration procedure is continued until eqs. 58 and 17 are satisfied. The solution gives the values of flow depths z_2, z_3, \dots, z_N and the discharge Q_N . The values of discharge in all other nodes are calculated according to the equation:

$$\begin{aligned}
Q_i = Q_N + \sum_{j=i}^{N-1} & \left[\frac{1}{2\Delta t} \frac{B_j + B_{j+1}}{2} \Delta x_j (z_j^{k+1} + z_{j+1}^{k+1} \right. \\
& \left. - z_{j+1}^k - z_j^k) - \frac{\Delta x_j}{2} (q_{j+1} + q_j) \right]
\end{aligned} \tag{63}$$

The calculated values of the flow depth and discharge are used as the initial conditions in the next time step.

Discharge Hydrograph as the Upper Boundary Condition

When the upper boundary condition is specified as the discharge hydrograph, the system of equations for the iteration procedure is given by eq. 48. The first row of the matrix is calculated according to eqs. 49-52. The other components are computed according to eqs. 23-47 with the exceptions given by eqs. 59-62. The function f_0 is calculated as follows:

$$f_o = Q_N - Q_1 + \sum_{j=1}^{N-1} \left[\frac{1}{2\Delta t} \frac{B_j + B_{j+1}}{2} \Delta x_j (z_j^{k+1} + z_{j+1}^{k+1} - z_{j+1}^k - z_j^k) - \frac{\Delta x_j}{2} (q_{j+1} + q_j) \right] \quad (64)$$

The iteration procedure continues until eqs. 58 and 17 are satisfied and the function f_o equals zero.

FINITE DIFFERENCE SOLUTION OF THE SAINT-VENANT EQUATIONS WITH LATERAL
OUTFLOW FROM A CHANNEL

The equations governing gradually varied, unsteady channel flow with lateral outflow from a channel may be written as follows (Strelkoff, 1969)

$$\frac{\partial Q}{\partial x} + B \frac{\partial z}{\partial t} - q = 0 \quad (65)$$

$$\frac{1}{8} \left(\frac{\partial Q}{\partial t} + \frac{Q}{A} \frac{\partial Q}{\partial x} \right) + \frac{\partial z}{\partial x} - S_o + S_f + \frac{Q \cdot q}{2A^2 g} = 0 \quad (66)$$

Multiplying eq. 65 by $Q/2A$ and eq. 66 by gA , and adding the results, we obtain

$$\frac{1}{gA} \left(\frac{\partial Q}{\partial t} + \frac{Q^2}{A} \frac{\partial}{\partial x} \right) - \frac{Q}{2gA^2} \left(\frac{\partial Q}{\partial x} + \frac{\partial A}{\partial t} \right) + \frac{\partial z}{\partial x} - S_o + S_f = 0 \quad (67)$$

Applying the finite difference approximation given by eqs. 6-8 leads to the set of equations

$$\begin{aligned}
G_i \equiv & Q_{i+1}^{k+1} - Q_i^{k+1} + \frac{B_{i+1}^{k+1} + B_i^{k+1}}{2} \frac{\Delta x_i}{2\Delta t} (z_{i+1}^{k+1} + z_i^{k+1} - z_{i+1}^k - z_i^k) \\
& - \frac{\Delta x_i}{2} (q_{i+1}^{k+1} + q_i^{k+1}) = 0
\end{aligned} \tag{68}$$

$$\begin{aligned}
F_i \equiv & z_{i+1}^{k+1} - z_i^{k+1} + \frac{\Delta x_i}{2} (S_{fi}^{k+1} + S_{fi+1}^{k+1} - S_{oi+1}^k - S_{oi}^k) \\
& + \frac{\Delta x_i}{q\Delta t(A_{i+1}^{k+1} + A_i^{k+1})} (Q_{i+1}^{k+1} + Q_i^{k+1} - Q_{i+1}^k - Q_i^k) \\
& + \frac{2}{g(A_{i+1}^{k+1} + A_i^{k+1})} \left[\frac{(Q_{i+1}^{k+1})^2}{A_{i+1}^{k+1}} - \frac{(Q_i^{k+1})^2}{A_i^{k+1}} \right] \\
& - \frac{(Q_{i+1}^{k+1})^2 - (Q_i^{k+1})^2}{2g[(A_{i+1}^{k+1})^2 + (A_i^{k+1})^2]} - \frac{\Delta x_i (Q_{i+1}^{k+1} + Q_i^{k+1})}{8g\Delta t[(A_{i+1}^{k+1})^2 + (A_i^{k+1})^2]} .
\end{aligned}$$

$$(B_{i+1}^{k+1} + B_i^{k+1}) \cdot (z_{i+1}^{k+1} + z_i^{k+1} - z_{i+1}^k - z_i^k) = 0 \tag{69}$$

To solve the system of equations given by eqs. 68 and 69 we utilize the Arno method and the Newton iterative procedure. The solution assumes the Manning equation as the lower boundary condition.

Discharge Hydrograph as the Upper Boundary Condition

When the discharge hydrograph is given as the upper boundary condition, the system of equations for the iteration procedure is given by eq. 48. the first row of the matrix is calculated according to eqs 49-52. the other components are calculated according to eqs. 23-47 with the following exceptions.

$$\frac{\partial F_i}{\partial A_i} = \left\{ \frac{\partial F_i}{\partial A_i} \right\}_{59} + \frac{2A_i^{k+1}}{[(A_{i+1}^{k+1})^2 + (A_i^{k+1})^2]^2} \cdot [\{ (Q_{i+1}^{k+1})^2 - (Q_i^{k+1})^2 \} / 2g + \frac{\Delta x_i}{8g\Delta t} (Q_{i+1}^{k+1} + Q_i^{k+1}) \cdot (B_{i+1}^{k+1} + B_i^{k+1}) \cdot (z_{i+1}^{k+1} + z_i^{k+1} - z_{i+1}^k - z_i^k)] \quad (70)$$

$$\frac{\partial F_i}{\partial A_{i+1}} = \left\{ \frac{\partial F_i}{\partial A_{i+1}} \right\}_{61} + \frac{2A_{i+1}^{k+1}}{[(A_{i+1}^{k+1})^2 + (A_i^{k+1})^2]^2} [\{ (Q_{i+1}^{k+1})^2 - (A_i^{k+1})^2 \} / 2g + \frac{\Delta x_i}{8g\Delta t} (Q_{i+1}^{k+1} + Q_i^{k+1}) \cdot (B_{i+1}^{k+1} + B_i^{k+1}) \cdot (z_{i+1}^{k+1} + z_i^{k+1} - z_{i+1}^k - z_i^k)] \quad (71)$$

$$\frac{\partial F_i}{\partial Q_{i+1}} = \left\{ \frac{\partial F_i}{\partial Q_{i+1}} \right\}_{60} + \frac{2Q_i^{k+1}}{2g[(A_{i+1}^{k+1})^2 + (A_i^{k+1})^2]} - \frac{\Delta x_i}{8g \Delta t [(A_{i+1}^{k+1})^2 + (A_i^{k+1})^2]} \cdot$$

$$(B_{i+1}^{k+1} + B_i^{k+1})(z_{i+1}^{k+1} + z_i^{k+1} - z_{i+1}^k - z_i^k) \quad (72)$$

$$\frac{\partial F_i}{\partial Q_{i+1}} = \left\{ \frac{\partial F_i}{\partial Q_{i+1}} \right\}_{62} - \frac{\Delta x_i}{2g[(A_{i+1}^{k+1})^2 + (A_i^{k+1})^2]} -$$

$$\frac{\Delta x_i}{8g \Delta t [(A_{i+1}^{k+1})^2 + (A_i^{k+1})^2]} \cdot (B_{i+1}^{k+1} + B_i^{k+1}) \cdot (z_{i+1}^{k+1} + z_i^{k+1} - z_{i+1}^k - z_i^k) \quad (73)$$

$$\frac{\partial F_i}{\partial z_i} = -1.0 - \frac{\Delta x_i (Q_{i+1}^{k+1} + Q_i^{k+1})}{8g \Delta t [(A_{i+1}^{k+1})^2 + (A_i^{k+1})^2]} (B_{i+1}^{k+1} + B_i^{k+1}) \quad (74)$$

$$\frac{\partial F_i}{\partial z_{i+1}} = 1.0 - \frac{\Delta x_i (Q_{i+1}^{k+1} + Q_i^{k+1})}{8g \Delta t [(A_{i+1}^{k+1})^2 + (A_i^{k+1})^2]} (B_{i+1}^{k+1} + B_i^{k+1}) \quad (75)$$

in which

$$\left\{ \frac{\partial T_i}{\partial A_i} \right\}_{59} \text{ is } \frac{\partial F_i}{\partial A_i} \text{ given by eq. 59}$$

$$\left\{ \frac{\partial F_i}{\partial A_{i+1}} \right\}_{61} \text{ is } \frac{\partial F_i}{\partial A_{i+1}} \text{ given by eq. 61}$$

$$\left\{ \frac{\partial F_i}{\partial Q_i} \right\}_{60} \text{ is } \frac{\partial F_i}{\partial Q_i} \text{ given by eq. 60}$$

$$\left\{ \frac{\partial F_i}{\partial Q_{i+1}} \right\}_{62} \text{ is } \frac{\partial F_i}{\partial Q_{i+1}} \text{ given by eq. 62}$$

The function f_0 is calculated according to eq. 64. The iteration procedure continues until eqs. 69 and 17 are satisfied and the function f_0 equals zero.

NUMERICAL RESULTS

In this section we present the results of stream flow simulation, which involves routing a triangular discharge hydrograph down a rectangular channel and is described by Viessman and others (1972, p. 197). Since no analytical solution is available, the results obtained by the method described herein are compared with the numerical results taken from Viessman and others (1972) who employed the explicit finite difference method.

In this case, a rectangular channel 6.1 m wide and 3.2 km long is carrying a steady uniform discharge $23.34 \text{ m}^3/\text{S}$ at 1.83 depth. The channel is

subjected to an upstream flood wave, which increases linearly from $23.34 \text{ m}^3/\text{S}$ to $57 \text{ m}^3/\text{S}$ in a period of 20 minutes, and then decreases linearly to $23.34 \text{ m}^3/\text{S}$ in 10 minutes. Hydraulic properties of the channel are $S_o = 0.0015 \text{ m/m}$, and $n = 0.02$. The purpose of the simulation is to predict the translation of the flood wave down the channel.

Viessman and others (1972) utilized in their simulation a 2-sec. time step and a 160-m spatial step. Herein, we retained spatial step of Viessman, and used 1-min., 5-min., and 10-min. time steps in order to investigate the influence of the time step size upon the accuracy of numerical results. We also investigated the influence of the lower boundary condition location. Beside that several calculations were done to show the model behavior in a case when groundwater inflow or outflow occurs. In the following paragraphs we describe the calculated cases.

Case 1: Time step size $\Delta t = 1 \text{ min.}$ The results of our numerical simulation and that of Viessman are shown in Figure 3 and 4. As it is seen there is a very good agreement between them.

Cases 2 and 3: Time step size $\Delta t = 5 \text{ min.}$ (Figs. 5 and 6) and $\Delta t = 10 \text{ min.}$ (Figs. 7 and 8). These results show that for larger time steps the simulated discharge and stage hydrographs are different from each other and different from those of Viessman, especially in regions of the hydrographs' large curvatures. However, it may be concluded that as long as a time-step size conforms to the shape of the hydrographs, the method should provide good accuracy of results.

Figure 3. Results for Case 1 using $\Delta t = 1$ min - discharge hydrographs.

- 1) upstream boundary condition ($x=0$); 2) $x = 1.6$ km; and
- 3) $x = 3.2$ km.

Solid line indicates results from the presented method

Dashed line indicates Viessman's results.

*

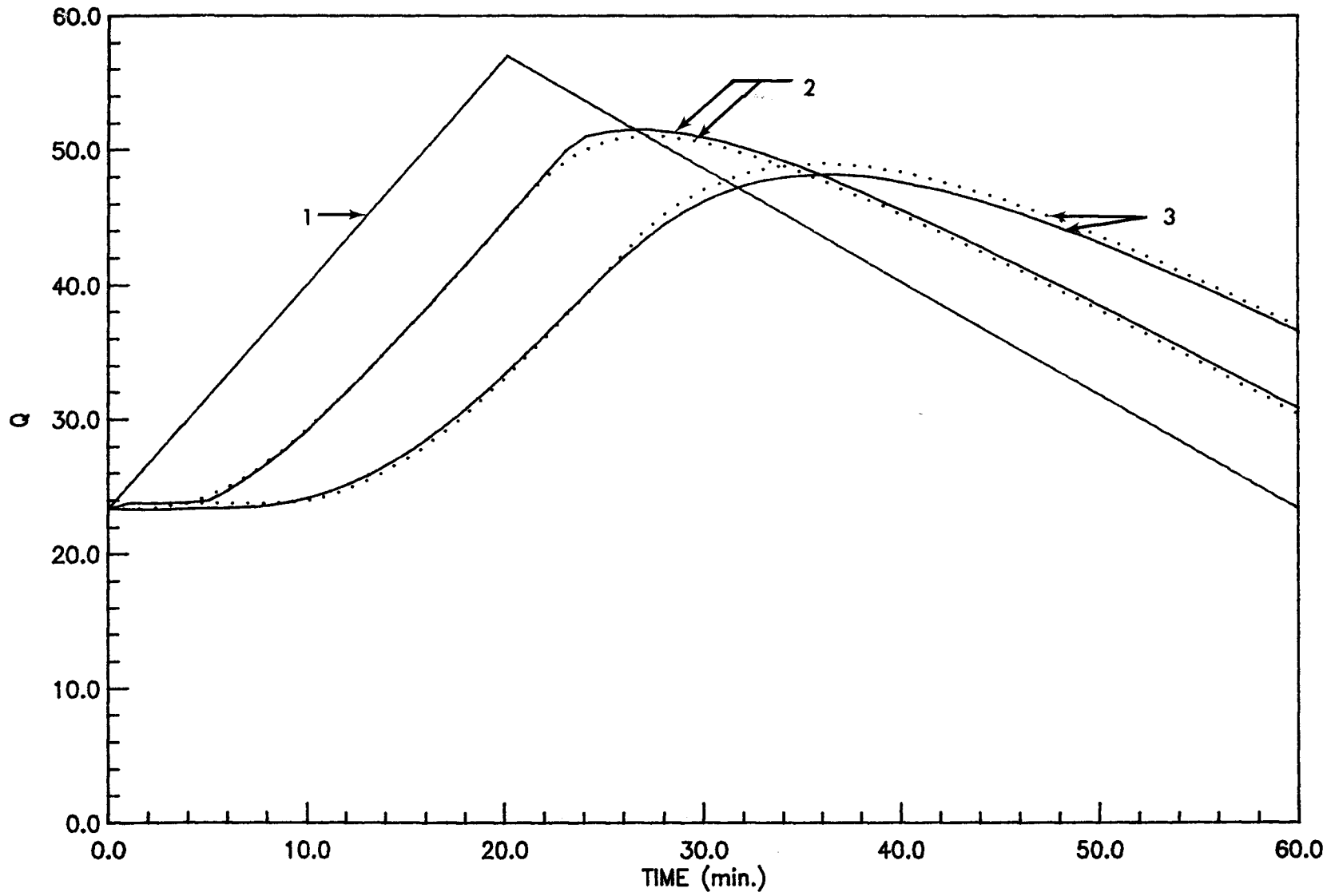


Figure 3

Figure 4. Results for Case 1 using $\Delta t = 1$ min - stage hydrographs.

* 1) $x = 1.6$ km and 2) $x = 3.2$ km

Solid line indicates results from the presented method

Dashed line indicates Viessman's results.

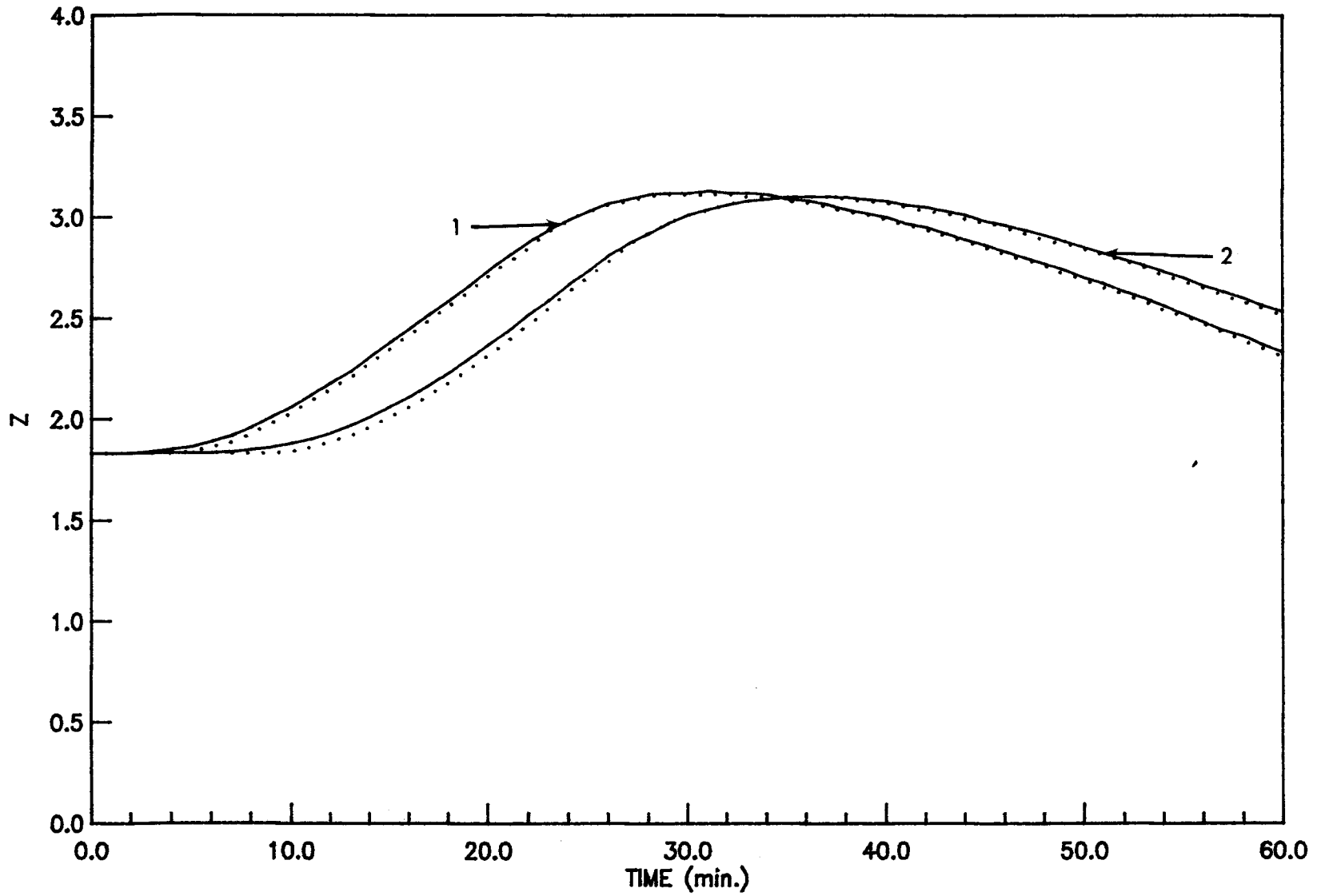


Figure 4

Figure 5. Results for Case 2 using $\Delta t = 5$ min - discharge hydrographs.

1) upstream boundary condition; 2) $x = 1.6$ km; and 3) $x = 3.2$ km.

Solid line indicates results from the presented method

Dashed line indicates Viessman's results.

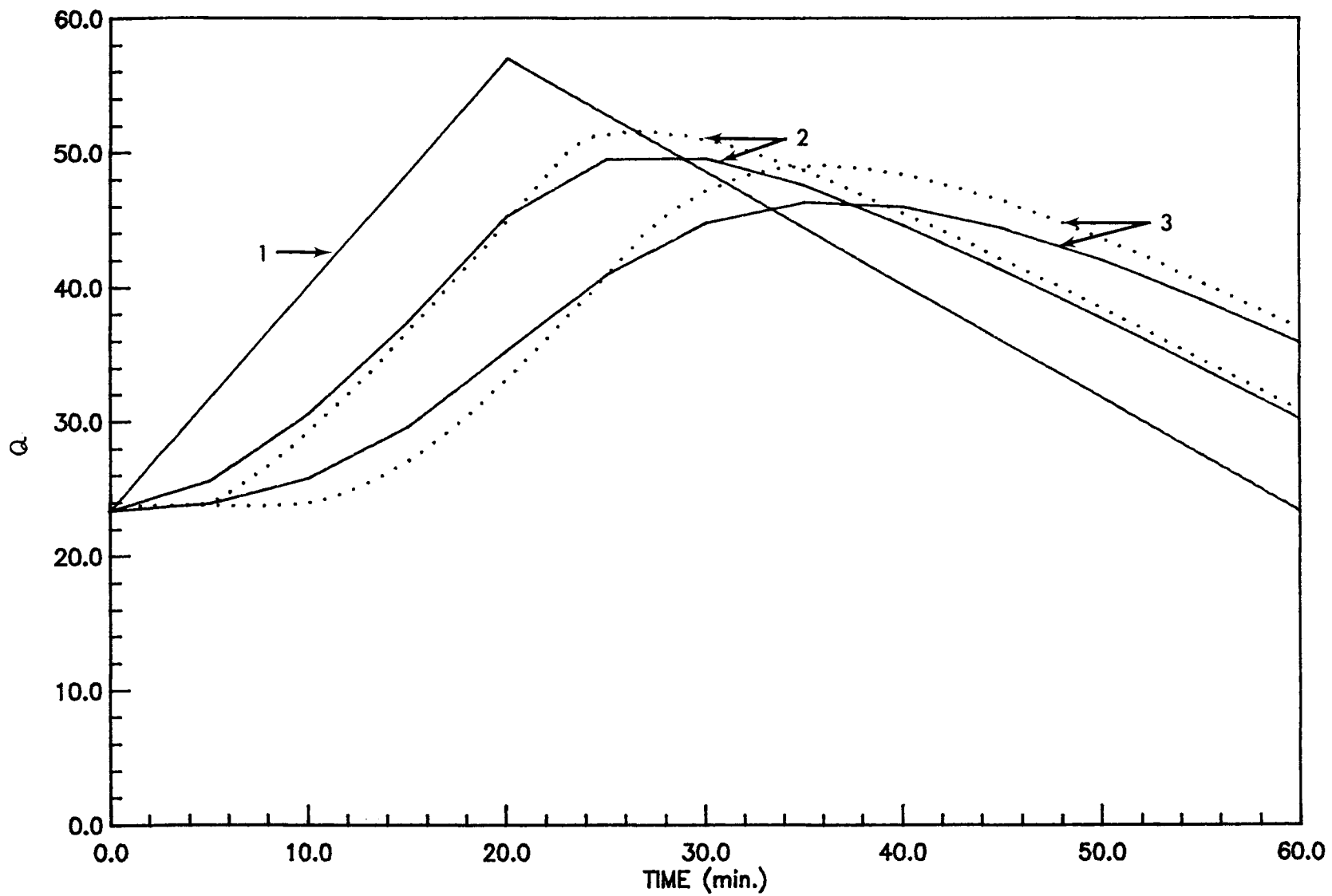


Figure 5

Figure 6. Results for Case 2 using $\Delta t = 5$ min - stage hydrographs.

1) $x = 1.6$ km and 2) $x = 3.2$ km.

Solid line indicates results from the presented method

Dashed line indicates Viessman's results.

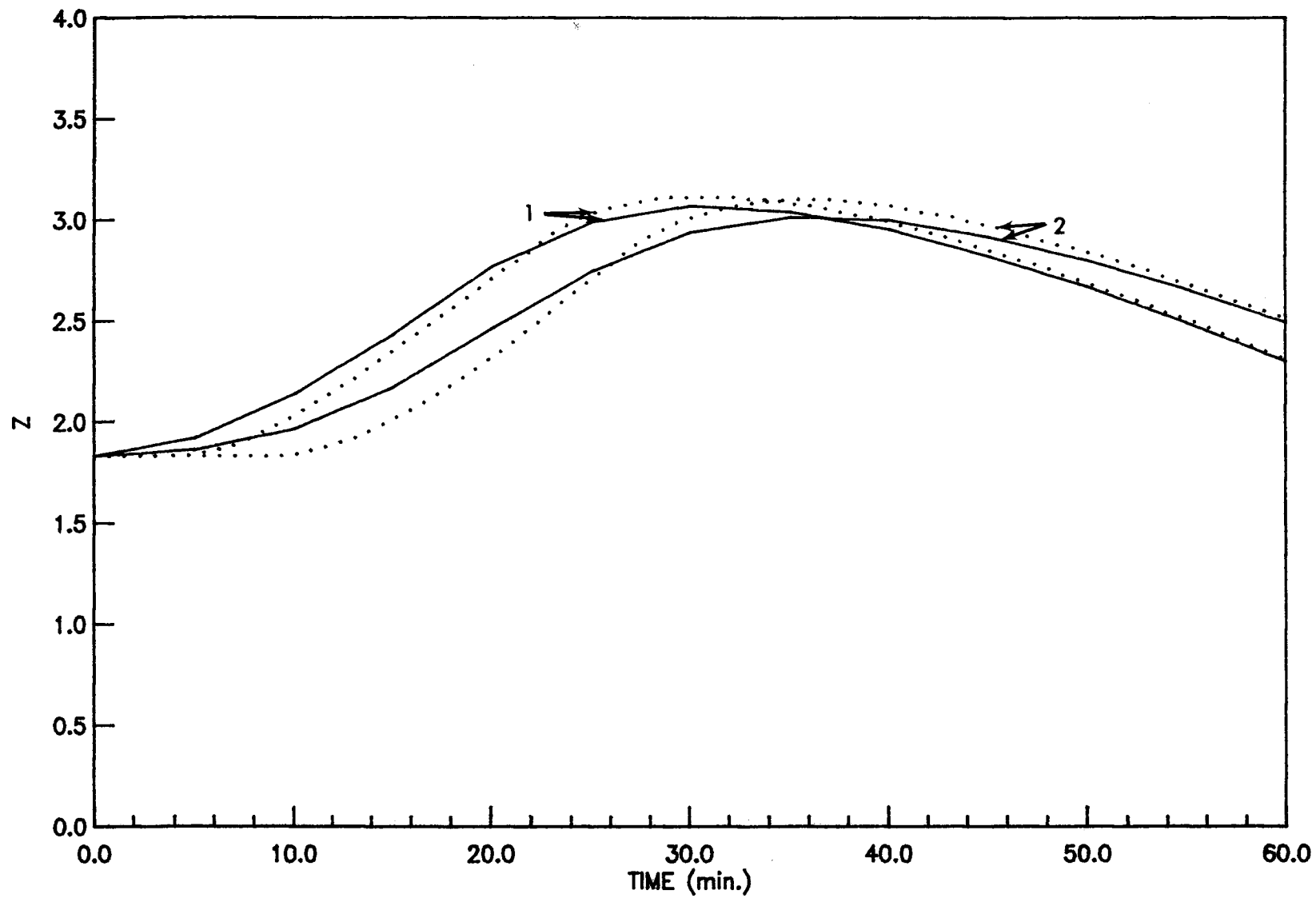


Figure 6

Figure 7. Results for Case 3 using $\Delta t = 10$ min - discharge hydrographs.

1) upstream boundary condition; 2) $x = 1.6$ km; and 3) $x = 3.2$ km.

Solid line indicates results from the presented method

Dashed line indicates Viessman's results.

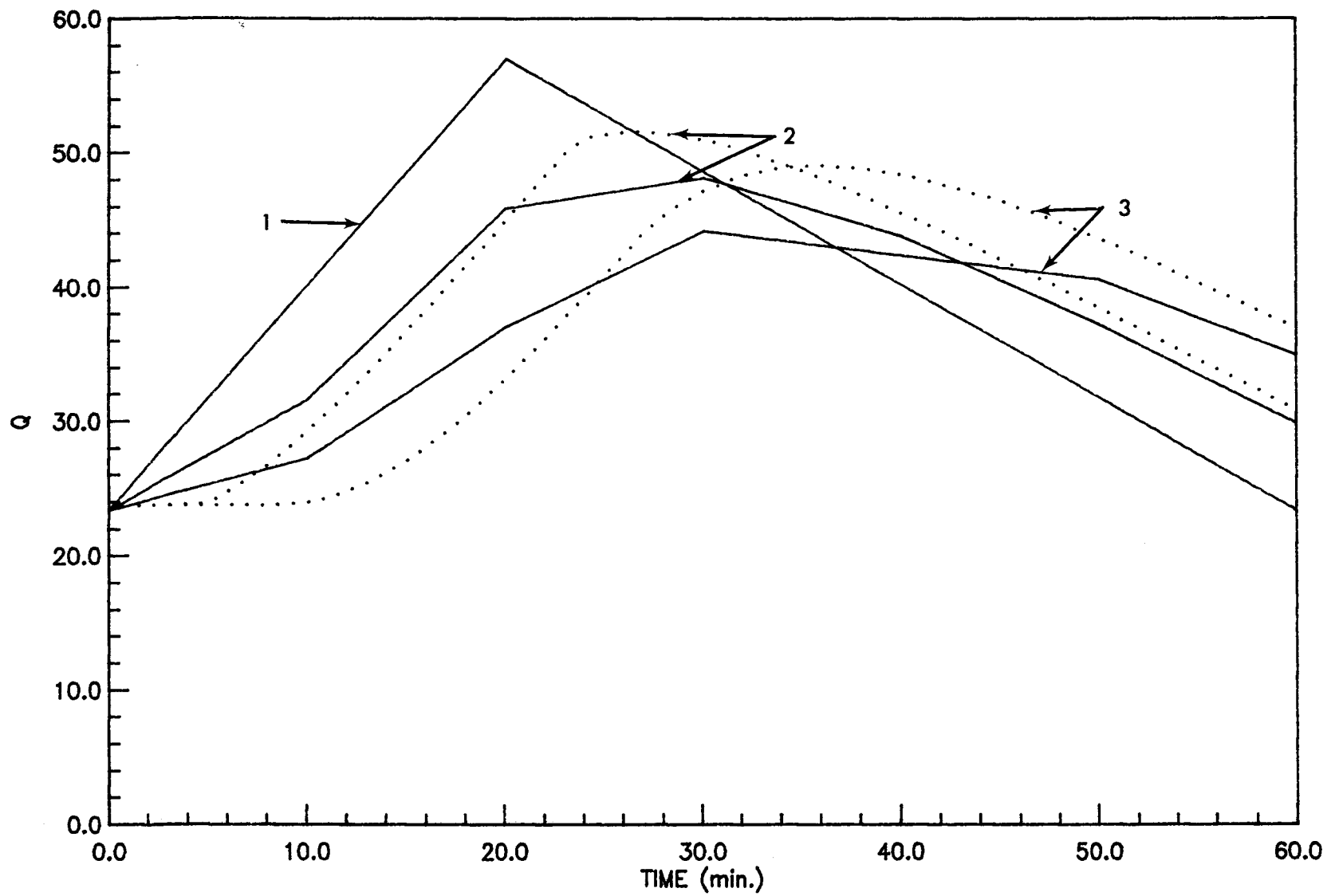


Figure 7

Figure 8. Results for Case 3 using $\Delta t = 10$ min - stage hydrographs.

1) $x = 1.2$ km and 2) $x = 3.2$ km.

Solid line indicates results from the presented method

Dashed line indicates Viessman's results.

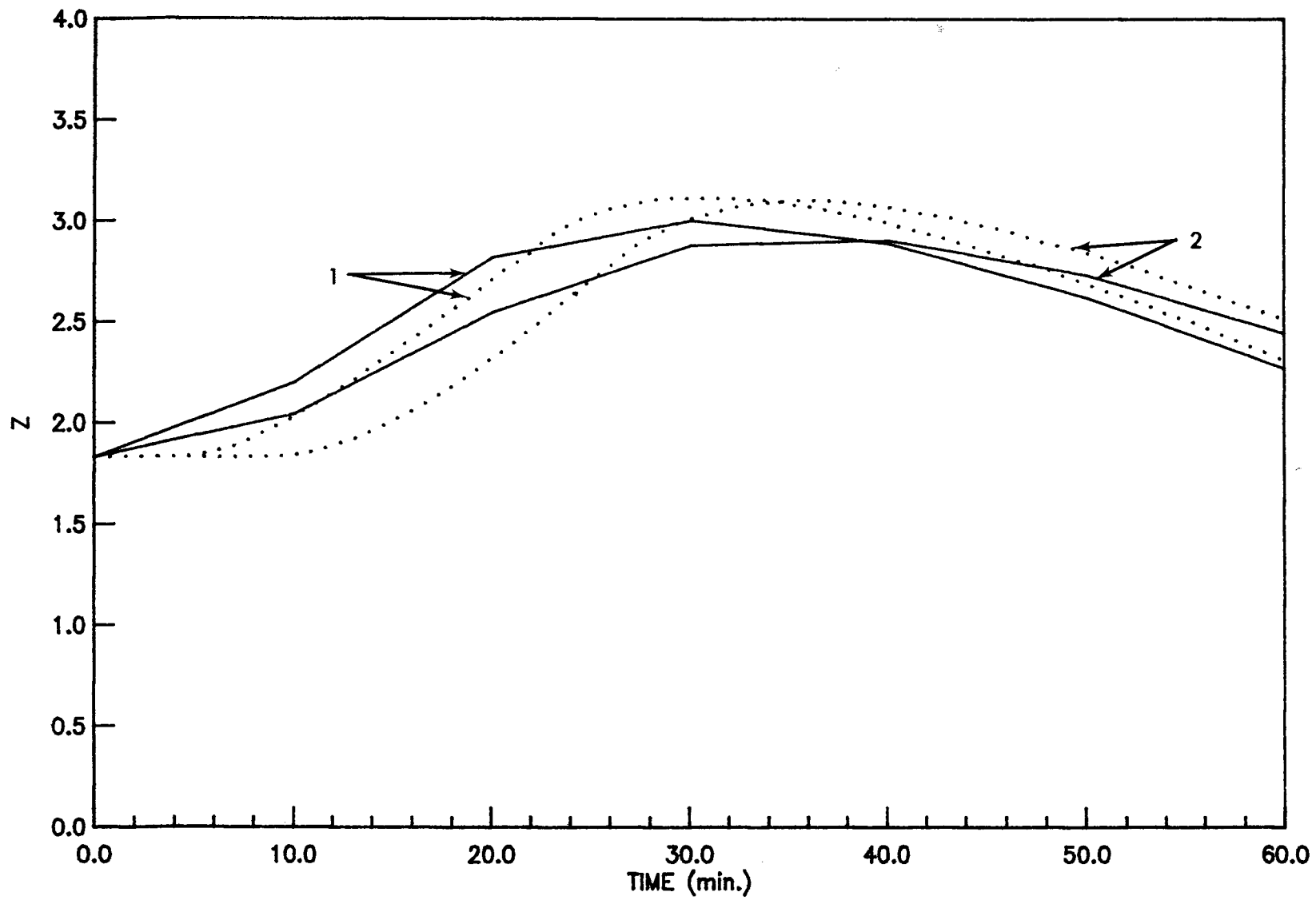


Figure 8

Case 4: In this case we investigated the influence of the lower boundary condition location on the numerical results. In order to do that the lower boundary condition was moved down the stream for 1.6 km. Thus, the whole length of the reach was 4.8 km. Figures 9 and 10 show the results for this case at $x = 1.6$ km and $x = 3.2$ km. The results at $x = 1.6$ km remained virtually the same, whereas the results at $x = 3.2$ km were different from those of Viessman. This behavior is caused by the influence of the lower boundary condition. When the lower boundary condition is resumed at $x = 3.2$ km, we force at this boundary a strict relationship between discharge and stage, given by the rating curve (Fig. 11). By moving the lower boundary condition down the stream we allow the stage-discharge relationship to have a form of hysteresis (Fig. 11), which is closer to the natural condition of stream flow. It may be concluded that for practical purposes, one should move the lower boundary condition down the stream from the reach under consideration in order to avoid the effect of this boundary condition on the prediction of results within the reach.

Case 5: In this case the stage hydrograph at $x = 0$, obtained as a result of computation for Case 1, was assumed as the upper boundary condition. The results (Figs. 12 and 13) are in good agreement with the simulation for discharge hydrograph as the upper boundary condition. This indicates that both types of boundary conditions may be used for numerical simulation.

Figure 9. Results for Case 4 - discharge hydrographs.

- 1) upstream boundary condition; 2) $x = 1.6$ km; and
- 3) $x = 3.2$ km.

Dashed line indicates results from the presented method obtained for the downstream boundary condition located at $x = 4.8$ km.

Solid line indicates Viessman's results obtained for the downstream boundary condition located at $x = 3.2$ km.

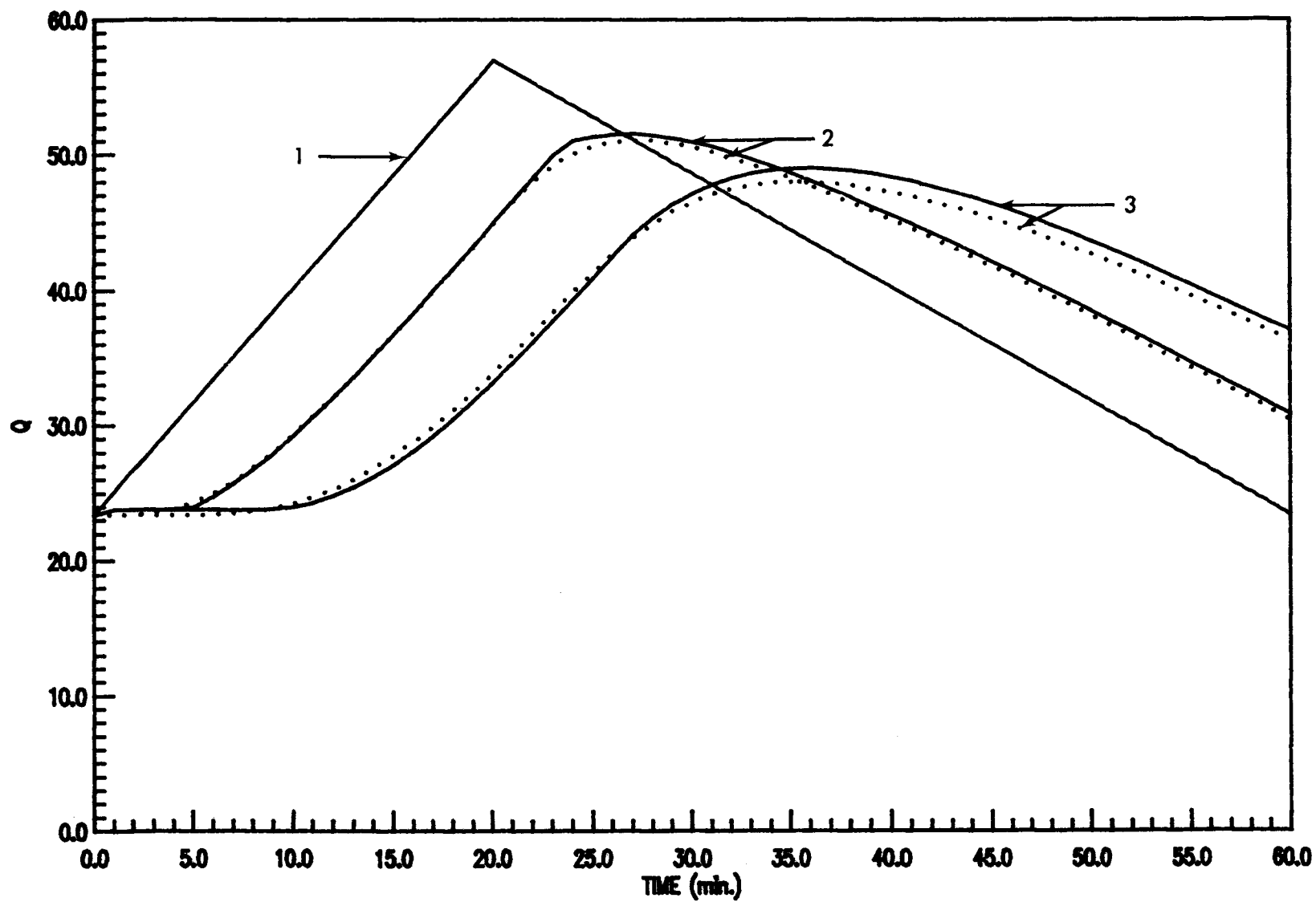


Figure 9

Figure 10. Results for Case 4 - stage hydrographs.

1) $x = 1.6$ km and 2) $x = 3.2$ km

Dashed line indicates results from the presented method obtained

for the downstream boundary condition located at $x = 4.8$ km.

Solid line indicates Viessman's results obtained for the

downstream boundary condition located at $x = 3.2$ km.

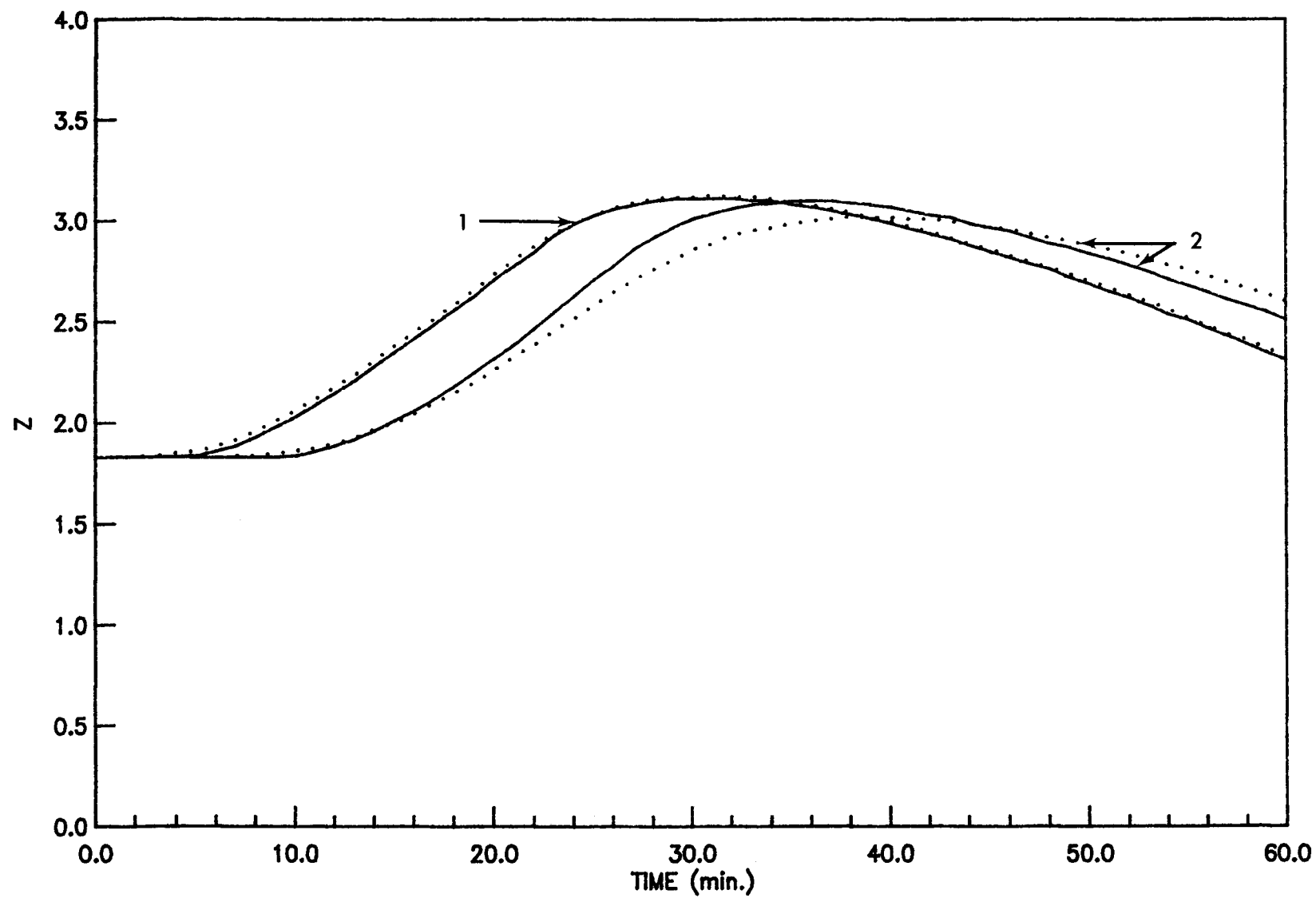


Figure 10

Figure 11. Discharge - stage relationship at $x = 3.2$ km for Case 4.

1) obtained from Viessman's results (Manning's formula);

2) obtained by the presented method for the downstream

boundary condition located at $x = 4.8$ km.

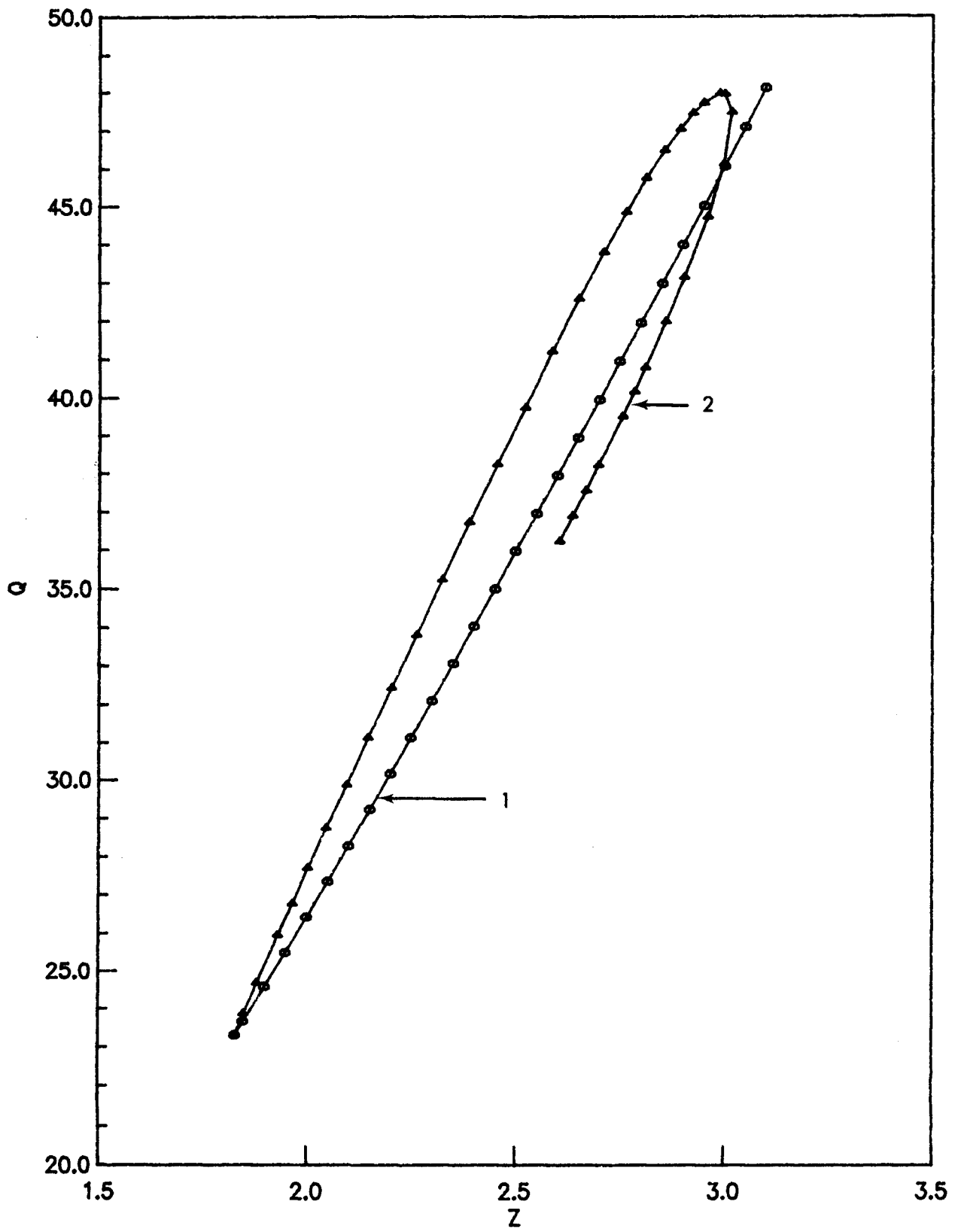


Figure 11

Figure 12. Results for Case 5 - discharge hydrographs.

1) $x = 1.6$ km and 2) $x = 3.2$ km

Dashed line indicates results from the presented method obtained for stage hydrograph as the upstream boundary condition.

Solid line indicates Viessman's results obtained for discharge hydrograph as the upstream boundary condition.

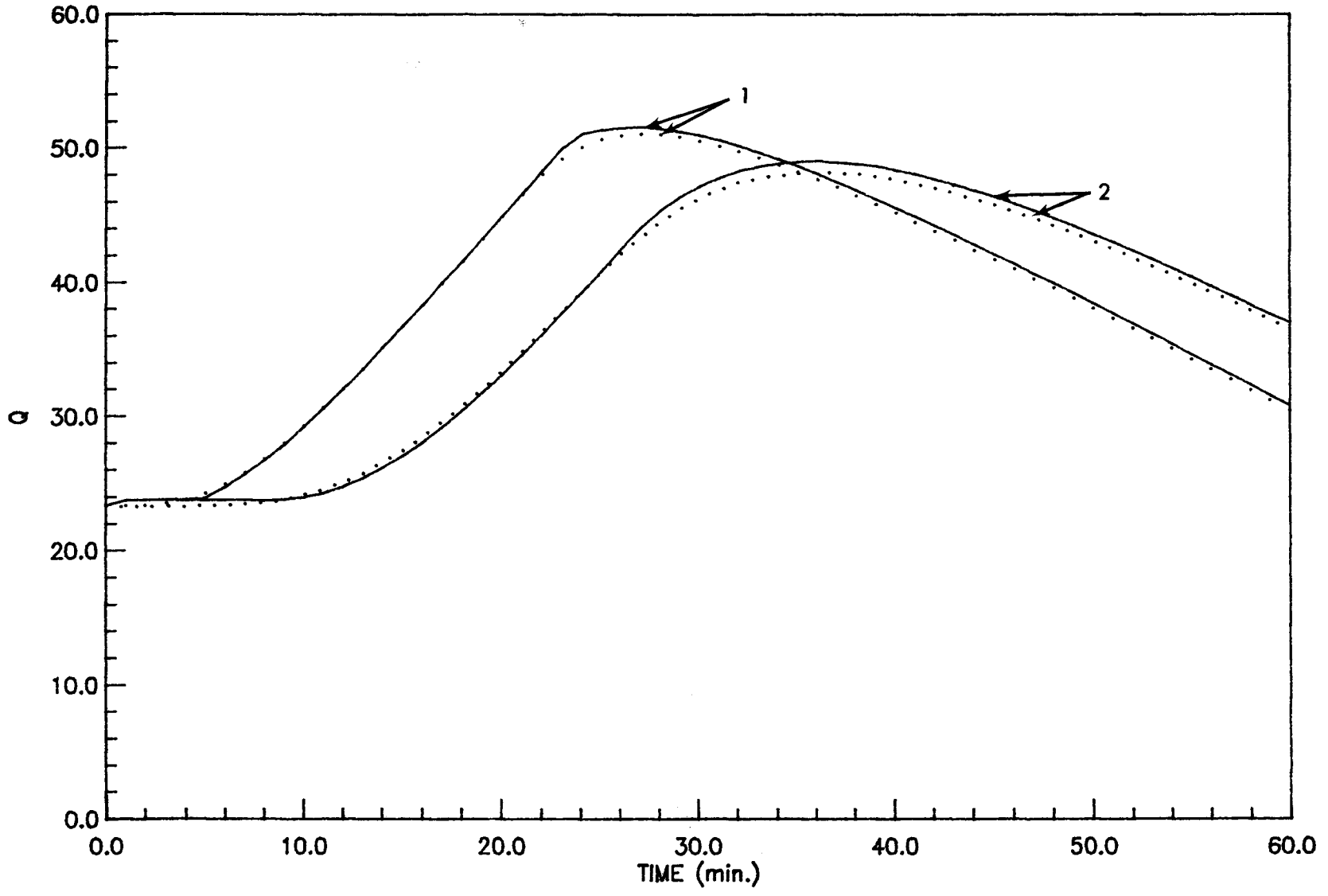


Figure 12

Figure 13. Results for Case 5 - stage hydrographs.

1) $x = 1.6$ km and 2) $x = 3.2$ km.

Dashed line indicates results from the presented method obtained for stage hydrograph as the upstream boundary condition.

Solid line indicates Viessman's results obtained for discharge hydrograph as the upstream boundary condition.

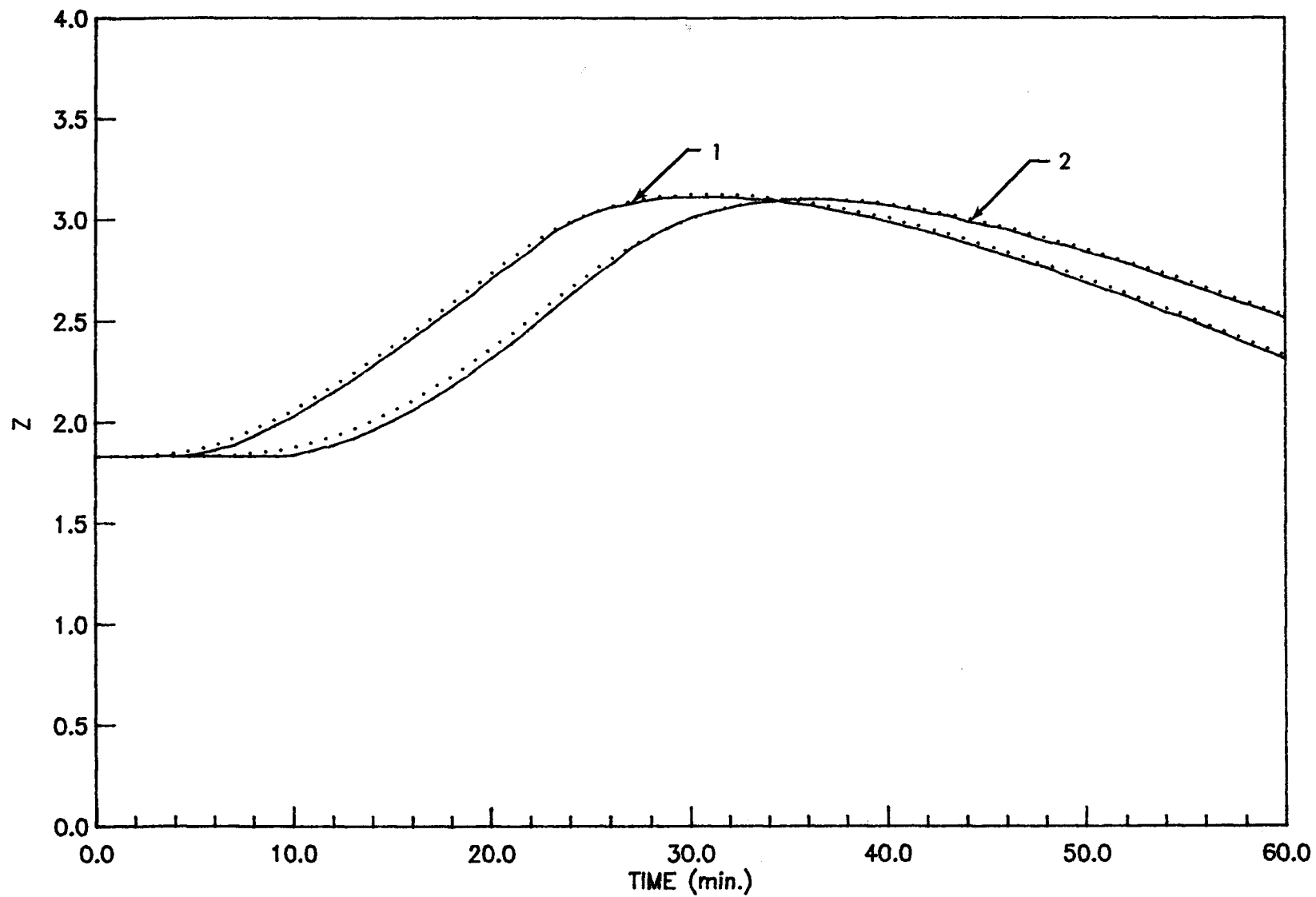


Figure 13

Cases 6-9: In order to show the behavior of the numerical stream flow model with lateral inflow or outflow, four simulations were run for the following values of lateral inflow or outflow: $q_1 = 0.002 \text{ m}^2/\text{sec.}$, $q_2 = 0.004 \text{ m}^2/\text{sec.}$, $q_3 = -0.002 \text{ m}^2/\text{sec.}$, $q_4 = -0.004 \text{ m}^2/\text{sec.}$ The total rates of inflow or outflow over the length of the stream (3.2 km) were $Q_1 = 6.4 \text{ m}^3/\text{S}$, $Q_2 = 12.8 \text{ m}^3/\text{S}$, $Q_3 = -6.4 \text{ m}^3/\text{S}$, $Q_4 = -12.8 \text{ m}^3/\text{S}$.

The initial conditions were the same as that of Case 1. The results of these simulations, presented in Figures 14-21, show important effect of the stream-aquifer interflow on the predicted stream and stage hydrographs, thus indicating the necessity of including stream-aquifer interaction component into a stream flow simulation model.

Case 10 and 11: Strelkoff (1969) gave different forms of the term which includes the effect of lateral inflow or outflow in the equation of motion (eq. 2), depending on the direction of flow (eq. 4). Cases 6-9 were calculated with regard to these distinctions (i.e., for inflow we assumed $D_L = Qq/(A^2g)$, and for outflow $D_L = Qq/(2A^2g)$). In order to check the effect of these different forms on numerical results, two computations were done, assuming D_L for outflow the same as for inflow (i.e., $D_L = Qq/(A^2g)$). The rates of outflow assumed were $q_1 = -0.002 \text{ m}^2/\text{sec.}$ (Case 10) and $q_2 = -0.004 \text{ m}^2/\text{sec.}$ (Case 11).

The comparison of the results for different forms of D_L are shown in Figures 22-25. As it may be seen, both forms produce almost the same results. Thus, it may be concluded that only one form of D_L may be used in stream-aquifer flow analysis. This fact should simplify future applications of the numerical model, since only one numerical procedure will be used for both inflow and outflow.

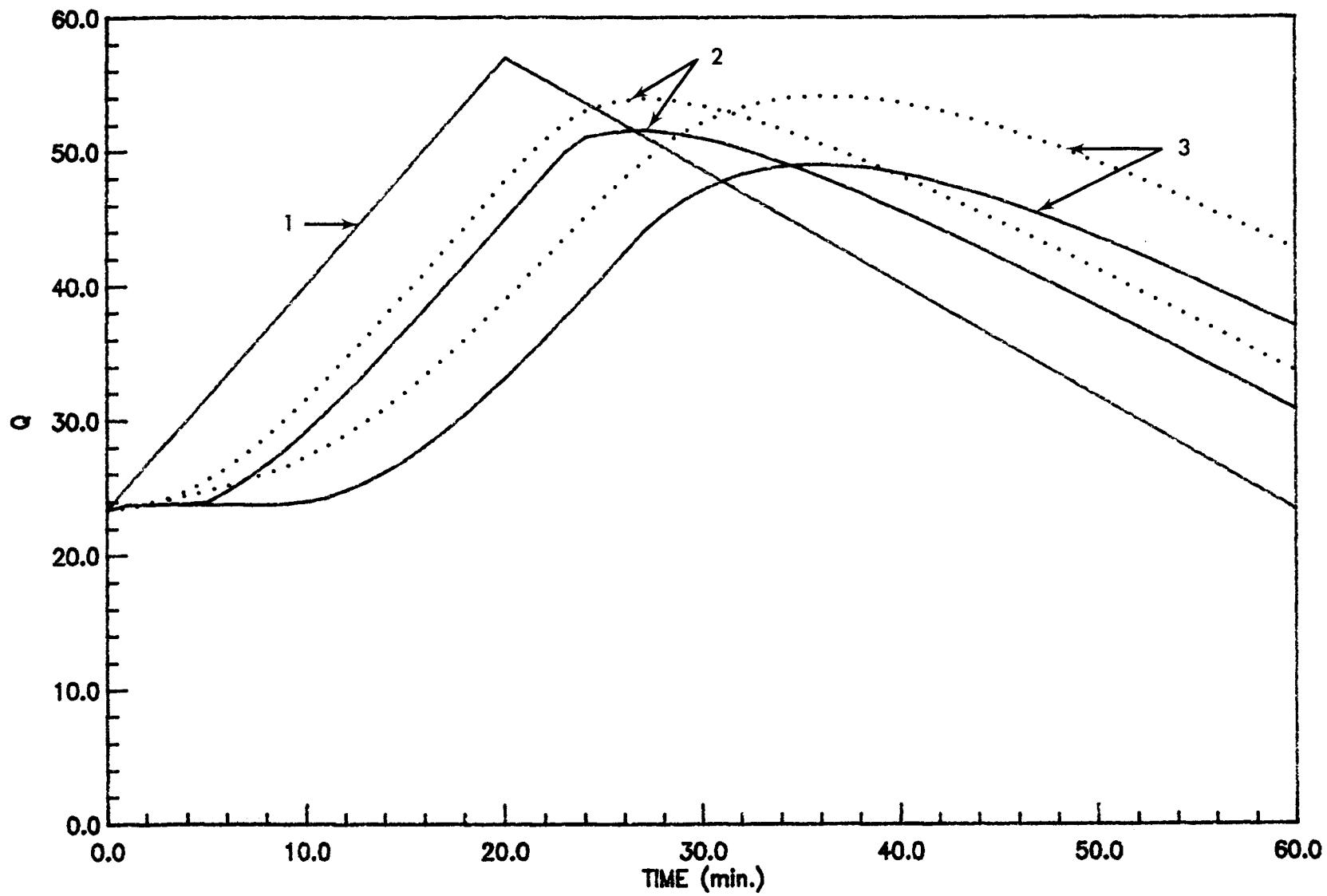


Figure 14

Figure 14. Results for Case 6 - discharge hydrographs.

1) upstream boundary condition; 2) $x = 1.6$ km; and

3) $x = 3.2$ km

Solid line indicates inflow $q = 0.0$ m²/sec.

Dashed line indicates inflow $q = 0.002$ m²/sec.

Figure 15. Results for Case 6 - stage hydrographs. 1) $x = 1.6$ km

and 2) $x = 3.2$ km

Solid line indicates inflow $q = 0.0$ m²/sec.

Dashed line indicates inflow $q = 0.002$ m²/sec.

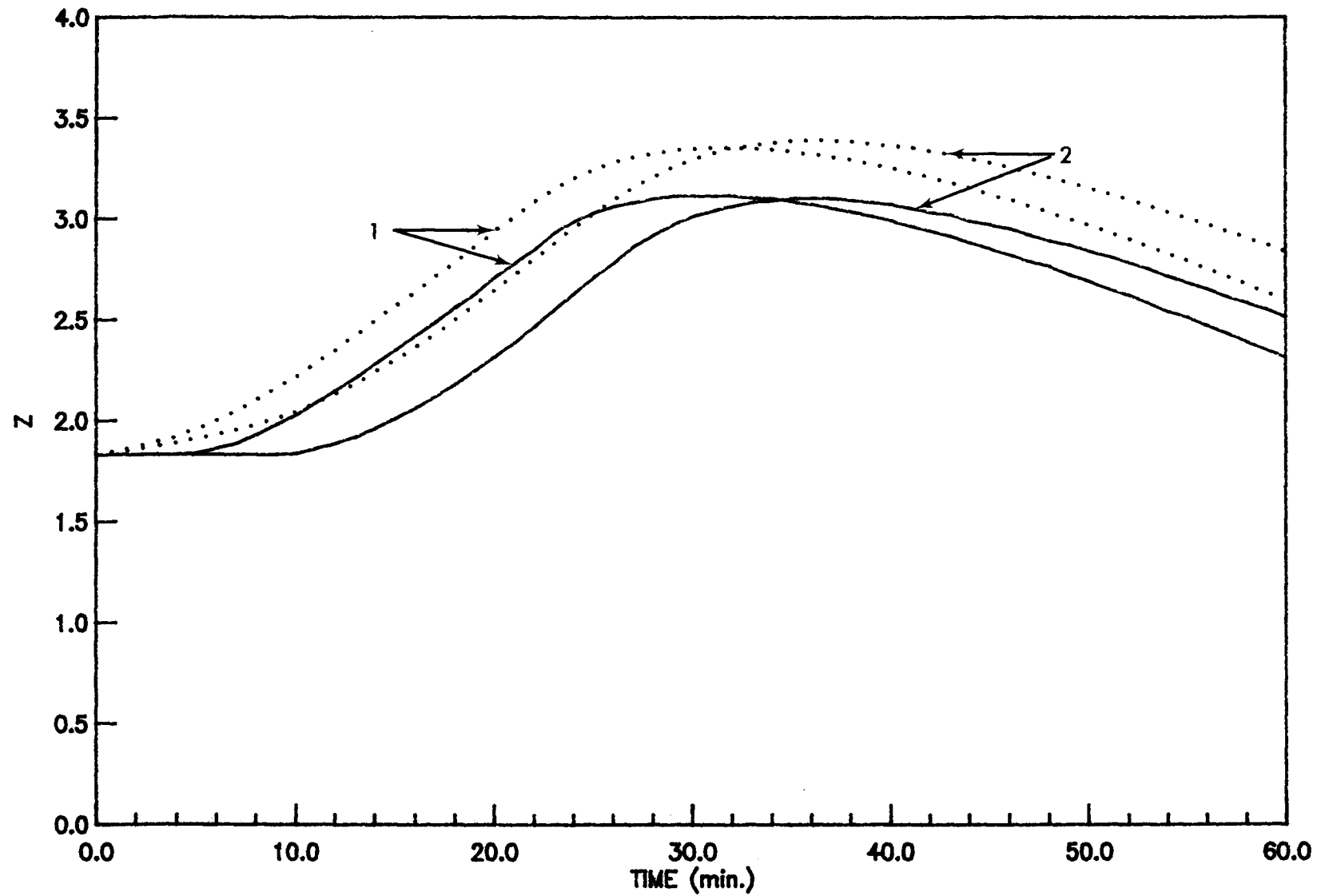


Figure 15

16
Figure 15. Results for Case 7 - discharge hydrographs. 1) upstream
boundary conditions; 2) $x = 1.6$ km; and 3) $x = 3.2$ km. ←
Solid line indicates inflow $q = 0.0$ m²/sec.
Dashed line indicates inflow $q = 0.004$ m²/sec.

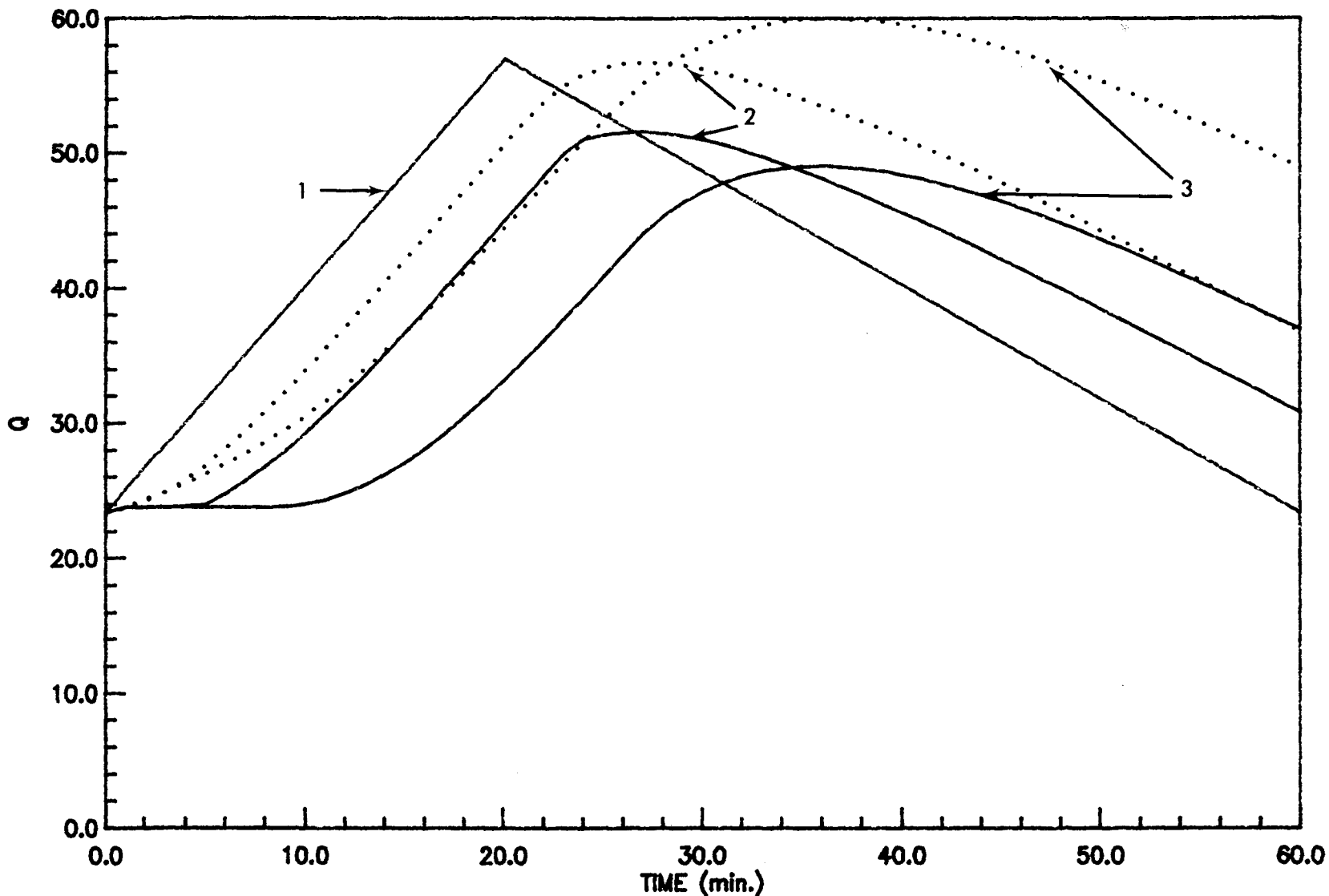


Figure 16

Figure 17. Results for Case 7 - stage hydrographs. 1) $x = 1.6$ km
and 2) $x = 3.2$ km.

Solid line indicates inflow $q = 0.0$ m²/sec.

Dashed line indicates inflow $q = 0.004$ m²/sec.

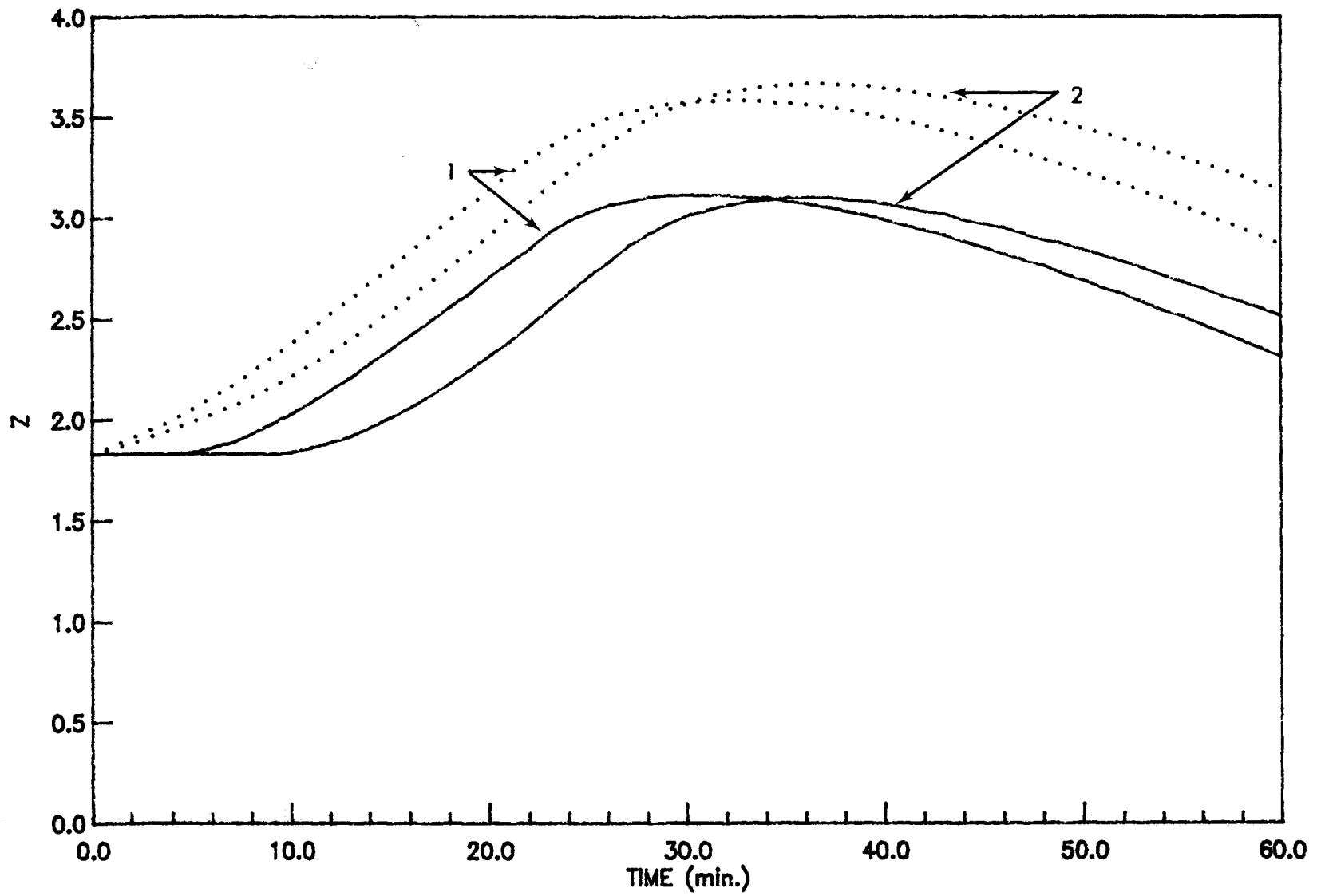


Figure 17

Figure 18. Results for Case 8 - discharge hydrographs. 1) upstream boundary condition; 2) $x = 1.6$ km; and 3) $x = 3.2$ km. Solid line indicates outflow $q = 0.0$ m²/sec. Dashed line indicates outflow $q = 0.002$ m²/sec.

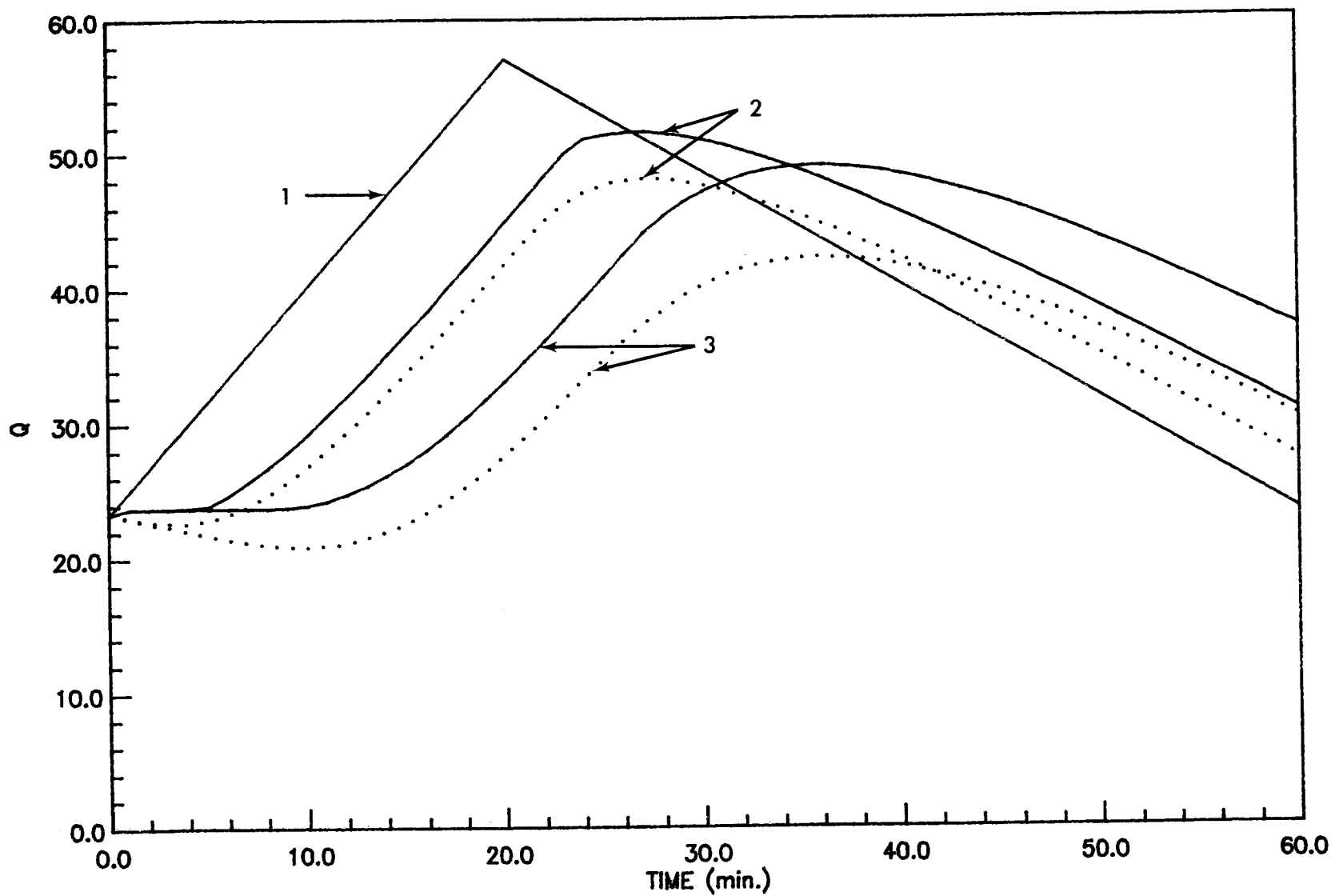


Figure 18

Figure 19. Results for Case 8 - stage hydrographs. 1) $x = 1.6$ km,
and 2) $x = 3.2$ km.

Solid line indicates outflow $q = 0.0 \text{ m}^2/\text{sec}$.

Dashed line indicates outflow $q = 0.002 \text{ m}^2/\text{sec}$.

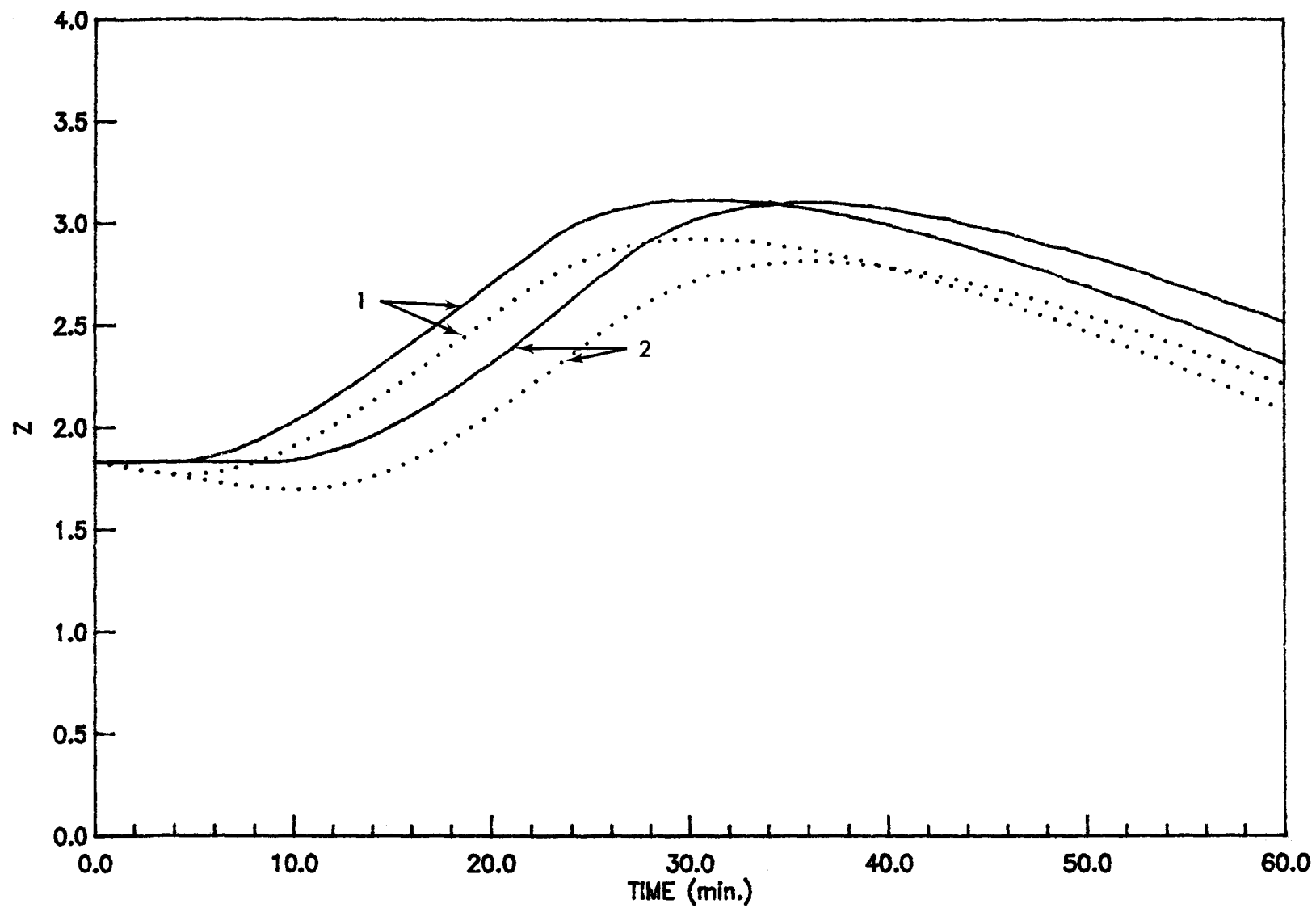


Figure 19

Figure 20. Results for Case 9 - discharge hydrographs. 1) upstream boundary condition; 2) $x = 1.6$ km; and 3) $x = 3.2$ km. Solid line indicates outflow $q = 0.0$ m²/sec. Dashed line indicates outflow $q = 0.004$ m²/sec.

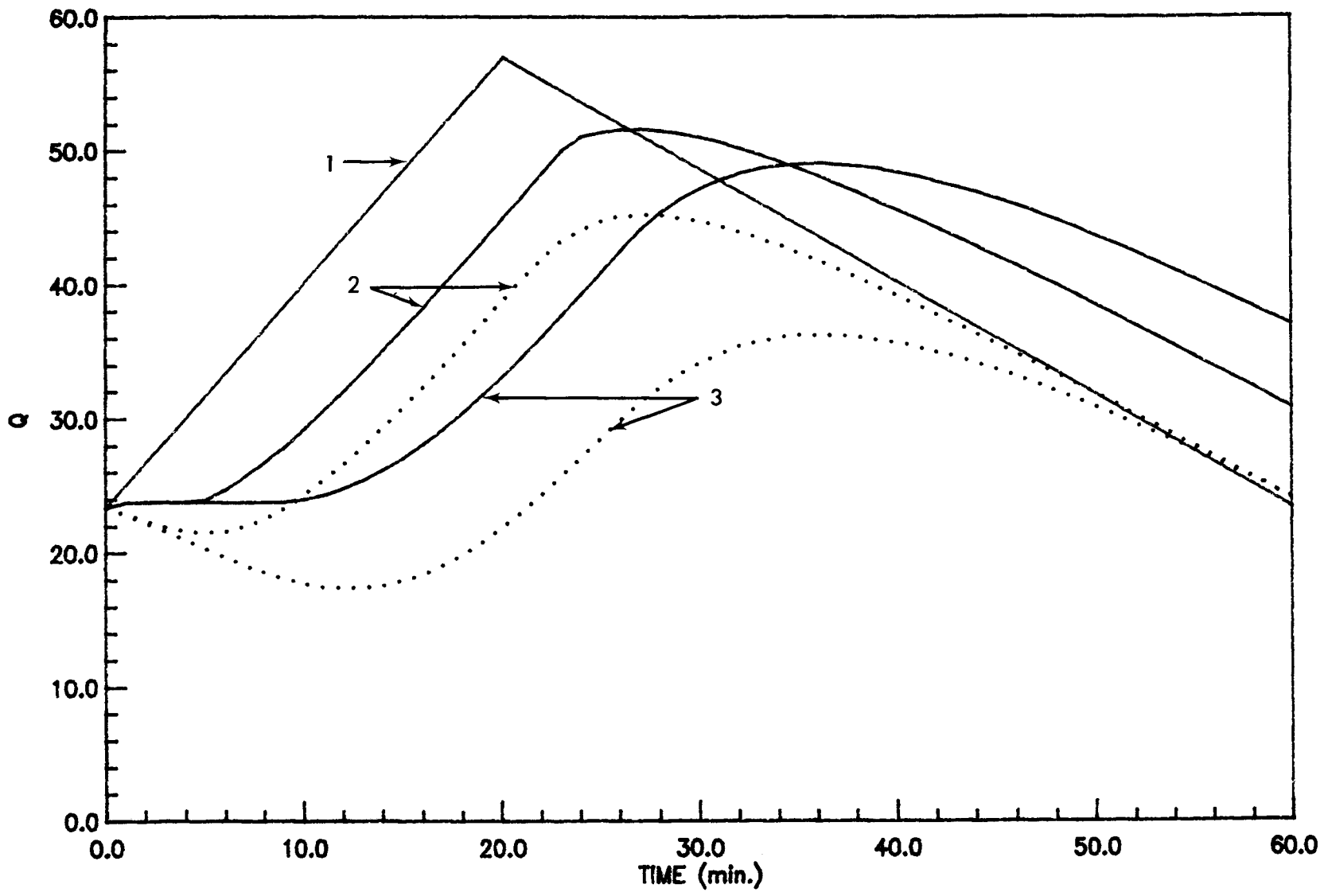


Figure 20

Figure 21. Results for Case 9 - stage hydrographs. 1) $x = 1.6$ km and

2) $x = 3.2$ km.

Solid line indicates outflow $q = 0.0$ m²/sec.

Dashed line indicates outflow $q = 0.004$ m²/sec.

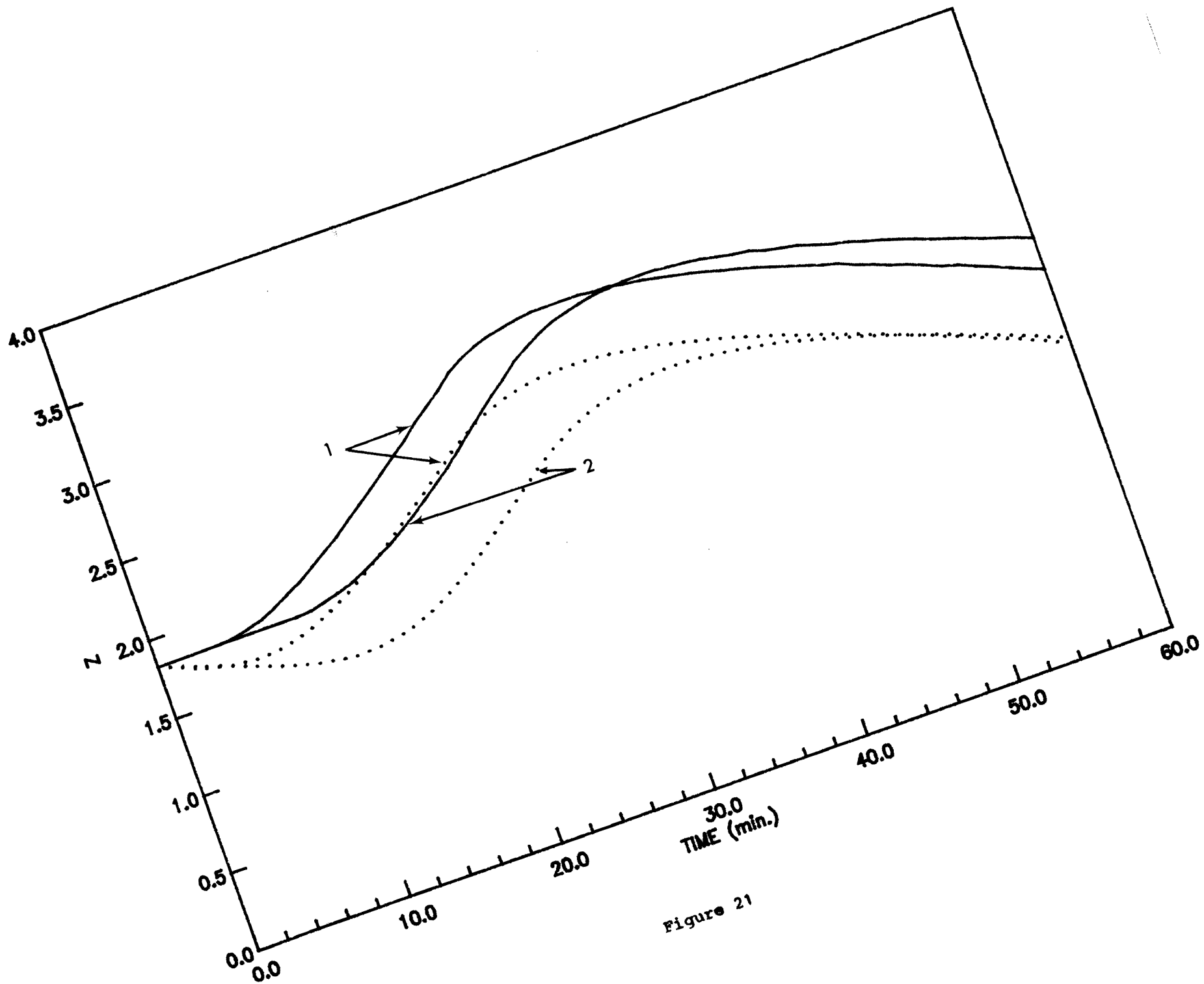


Figure 21

Figure 22. Results for Case 10 - discharge hydrographs. 1) $x = 1.6$ km;

2) $x = 3.2$ km.

Solid line indicates $D_L = Qq/A^2g$

Dashed line indicates $D_L = Qq/2A^2g$

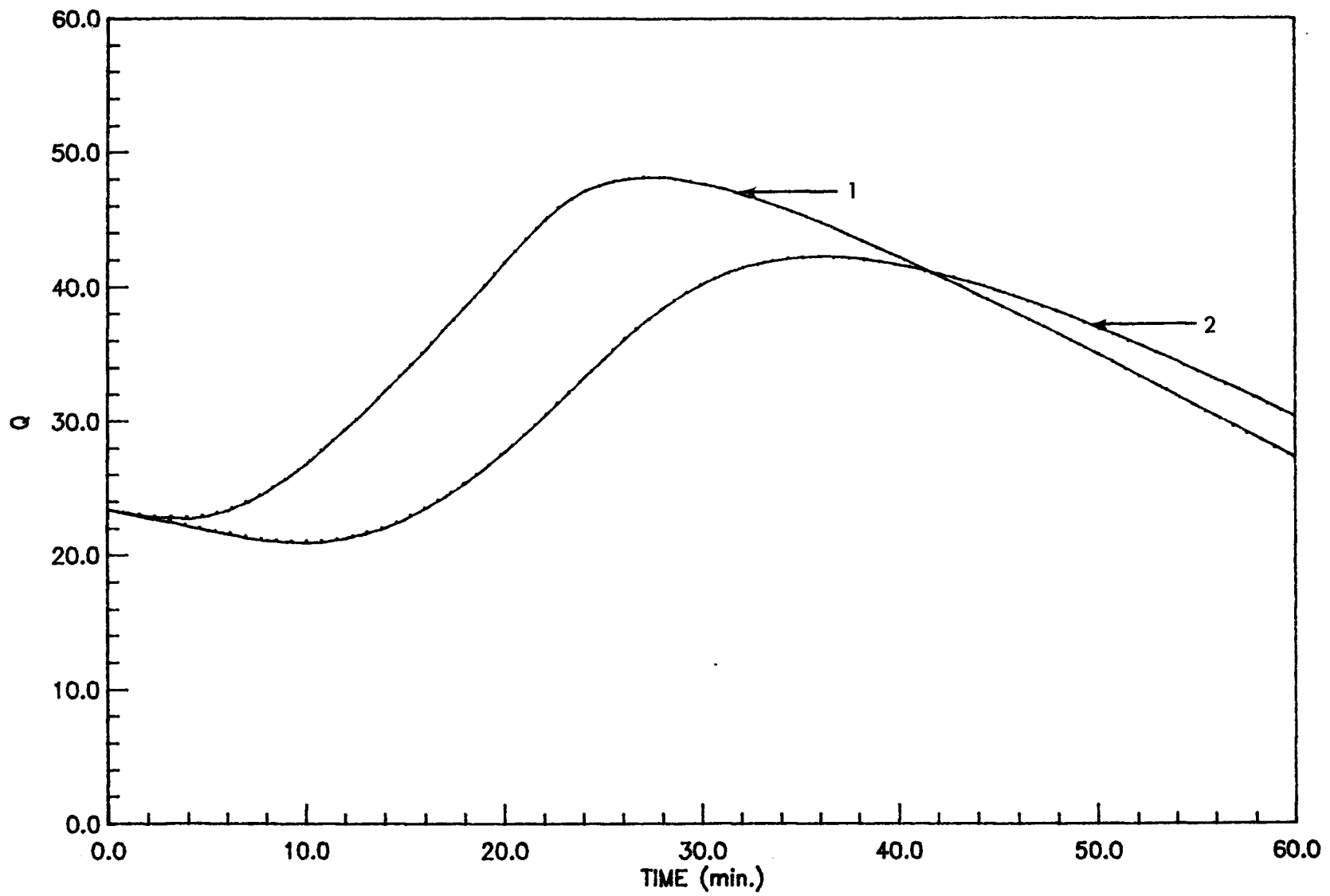


Figure 22

Figure 23. Results for Case 10 - stage hydrographs. 1) $x = 1.6$ km;

2) $x = 3.2$ km.

Solid line indicates $D_L = Qq/A^2g$

Dashed line indicates $D_L = Qq/2A^2g$

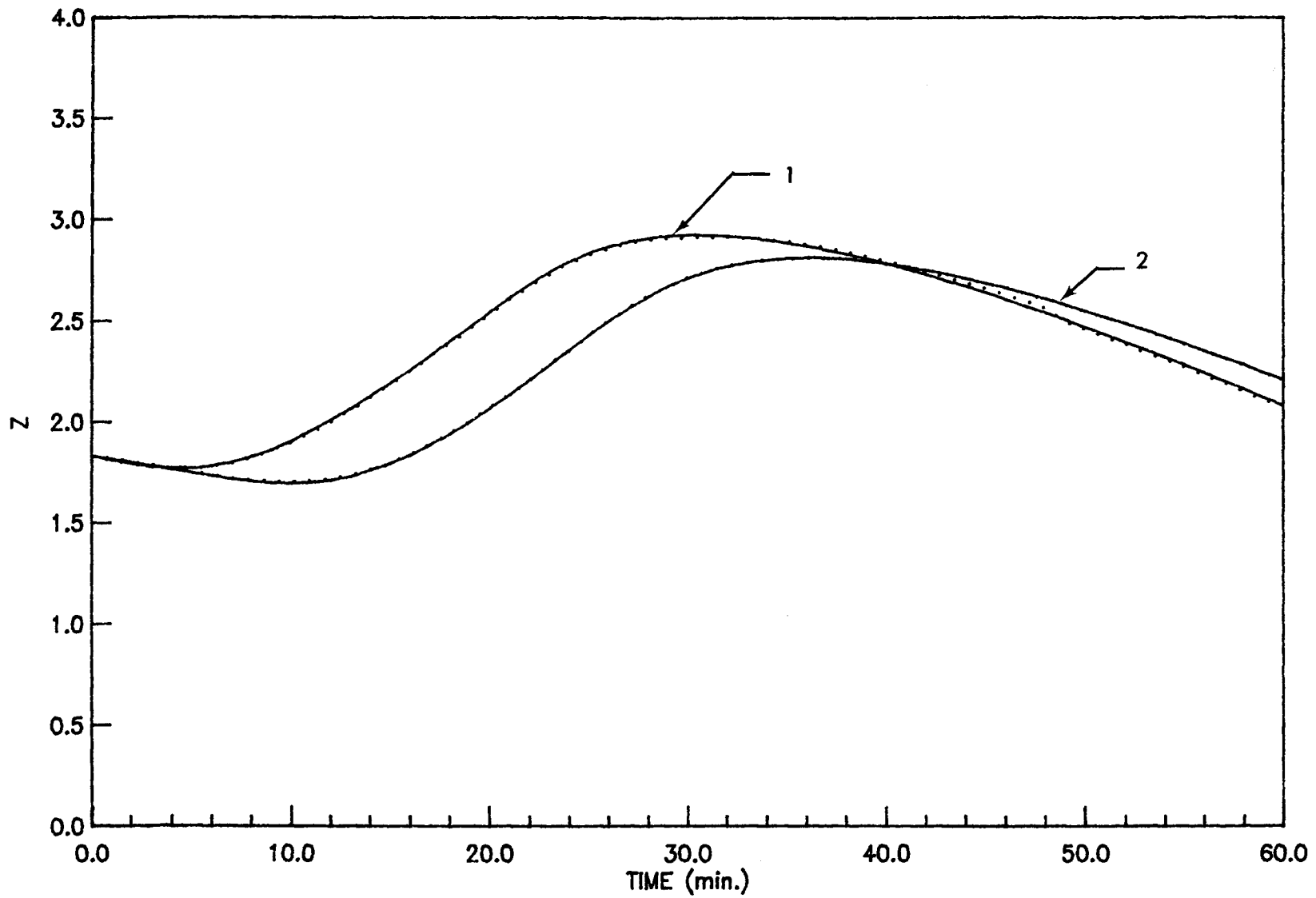


Figure 23

Figure 24. Results for Case 11 - discharge hydrographs. 1) $x = 1.6$ km;

2) $x = 3.2$ km.

Solid line indicates $D_L = Qq/A^2g$

Dashed line indicates $D_L = Qq/2A^2g$

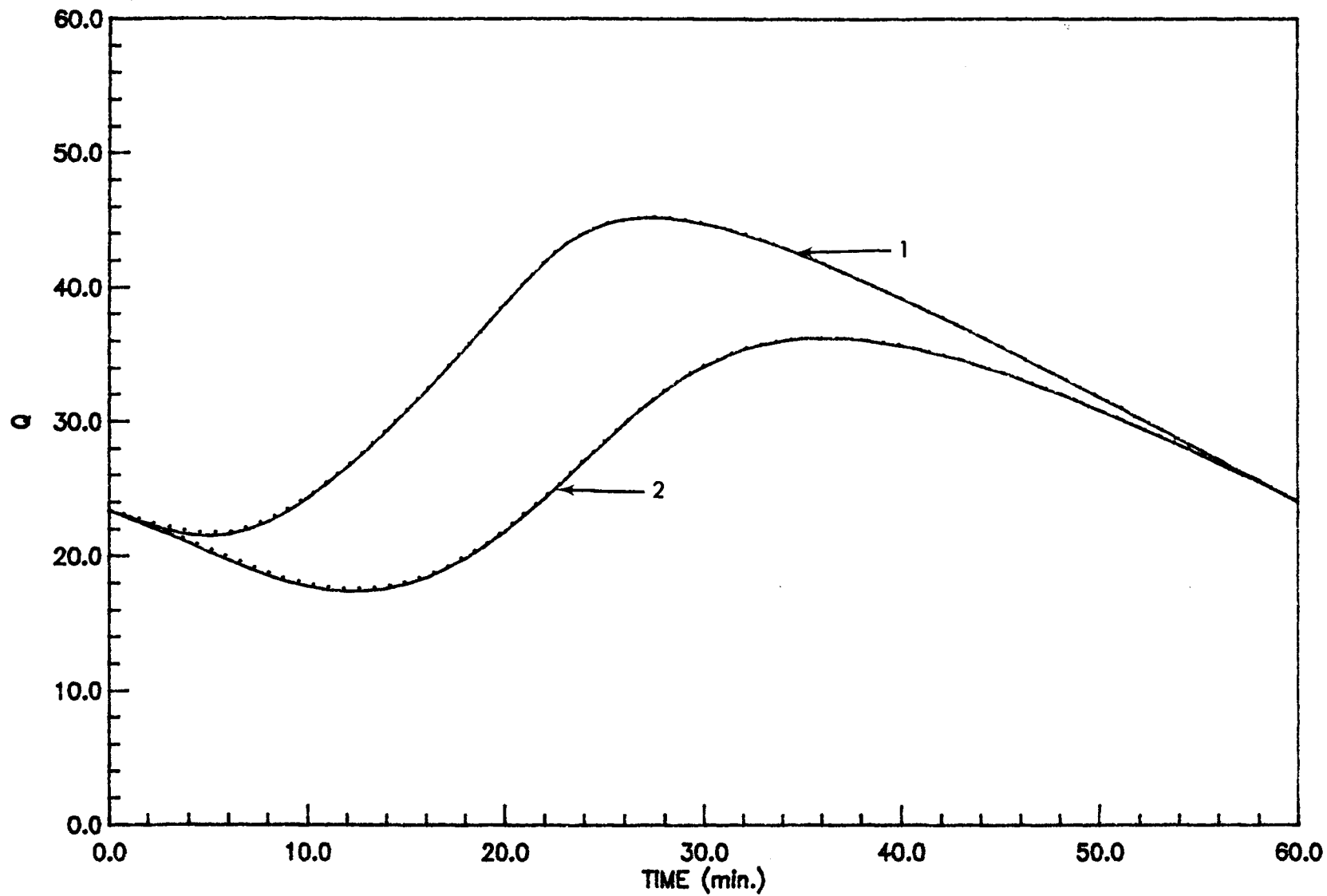


Figure 24

Figure 25. Results for Case 11 - stage hydrographs. 1) $x = 1.6$ km;

2) $x = 3.2$ km.

Solid line indicates $D_L = Qq/A^2g$

Dashed line indicates $D_L = Qq/2A^2g$

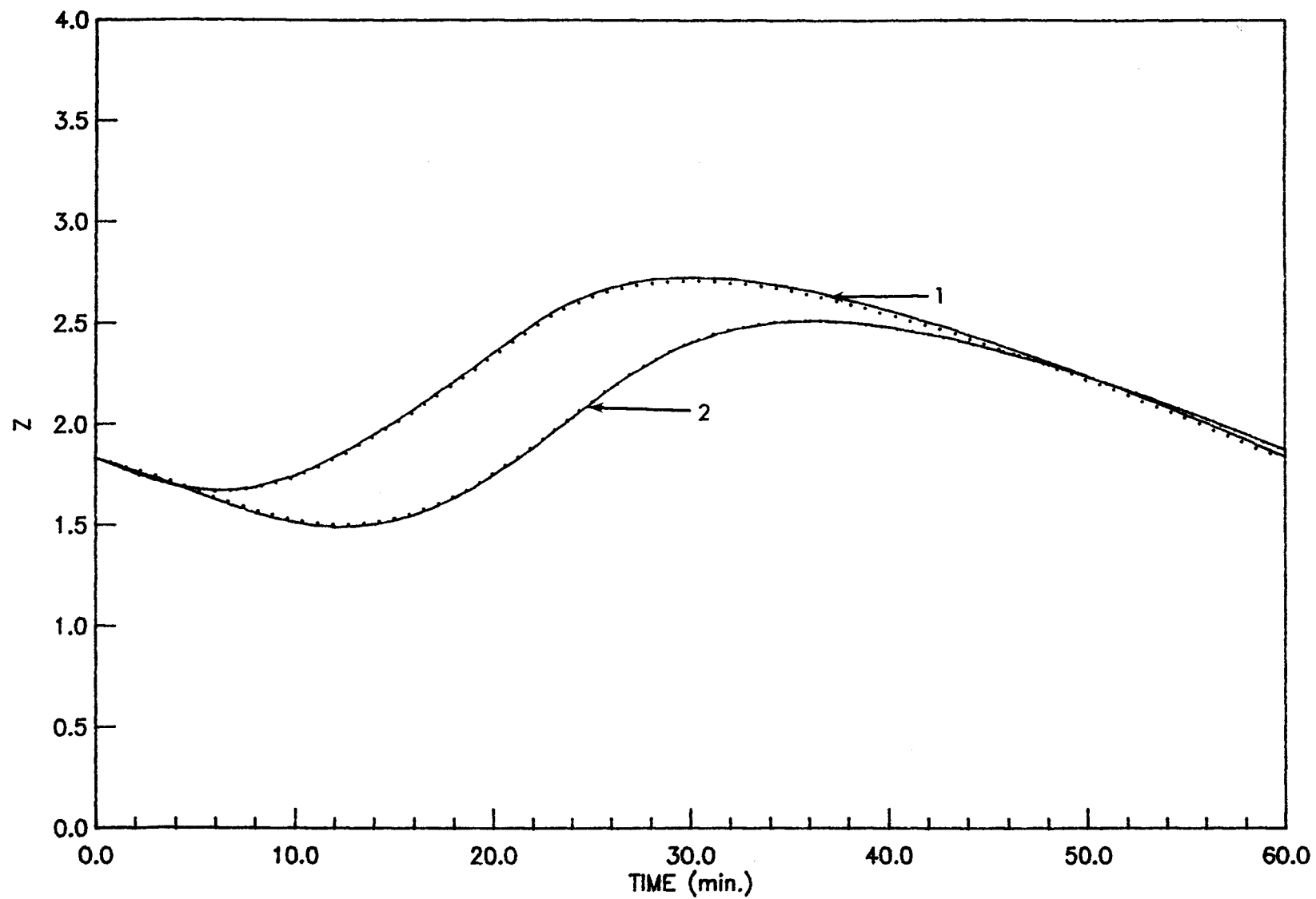


Figure 25

REFERENCES

- Chow, V.T., 1959, Open-channel hydraulics: New York, McGraw-Hill, 680 p.
- Cooley, R.L., and Moin, S.A., 1976, Finite element solution of Saint-Venant equations: Journal of the Hydraulics Division, ASCE, HY6, pp. 759-775.
- Cunningham, A.B., 1977, Modeling and analysis of hydraulic interchange of surface and groundwater: Technical Report Series H-W, No. 34, Desert Research Institute, University of Nevada, 89 p.
- Freeze, R.A., 1972, Role of subsurface flow in generating surface runoff. 1. base flow contributions to channel flow: Water Resources Research, vol. 8, no. 3, pp. 609-623.
- Greco, F. and Panottoni, L., 1977, Numerical solution of the St. Venant equations: in Cirian, T.A., et al. (eds.), Mathematical models for surface water hydrology: New York, John Wiley, pp. 181-194.
- Henderson, F.M., 1966, Open channel flow: New York, Macmillan, 522 p.
- Macon, N., 1963, Numerical analysis: New York, John Wiley, 161 pp.
- Stelkoff, Th., 1969, One dimensional equation of open-channel flow: Journal of Hydraulics Division, ASCE, vol. 95, no. HY3, pp. 861-875.
- Viesman, W., Harbaugh, T.E., and Knapp, J.W., 1972, Introduction to hydrology: New York, Intext Educational Publishers, 415 p.